The 8th International Conference on Hadron Spectrosopy
BEIJING, August 24 – 28, 1999

Results From Deep Inelastic Scattering at HERA

Jim Whitmore
(Penn State University)

on behalf of the ZEUS and H1 Collaborations

Studies of EW physics, NLO pQCD tests, the structure of the proton and the structure of diffraction

Overview

Introduction

- Kinematics of Deep Inelastic Scattering
- Cross sections and structure functions

Structure functions at high, medium and low Q^2

- Overview of $F_2 \Rightarrow$ Gluon
- High Q^2: study of electroweak effects ($e^{\pm}p$)
- Low Q^2: extrapolation to $\sigma_{\rm tot}^{\gamma p}$

Inclusive and exclusive diffraction

- Inclusive measurements $\Rightarrow$ Gluon (in diffraction)
- Exclusive vector meson production $\Rightarrow$ Scales
- Deeply Virtual Compton Scattering (DVCS)

Heavy quark and jet production (pQCD tests)

- F_2^c measurement $\Rightarrow$ Gluon
- Dijet production in DIS $\Rightarrow$ Gluon

Conclusions – what we will see is:

- Electroweak physics in DIS is in good agreement with the SM
- HERA data agree with NLO QCD principles
- Get a consistent gluon from several processes
- Low Q^2 and diffractive phenomena are probing the transition between soft physics and pQCD – issue of scales

Running at HERA

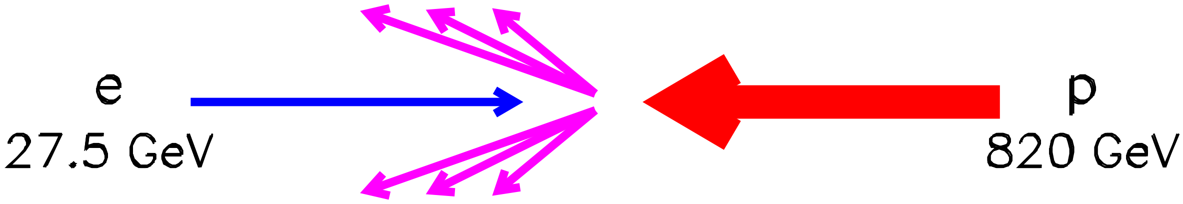

$\sqrt{s} = 300$ GeV

→ equivalent to 50 TeV fixed target energy

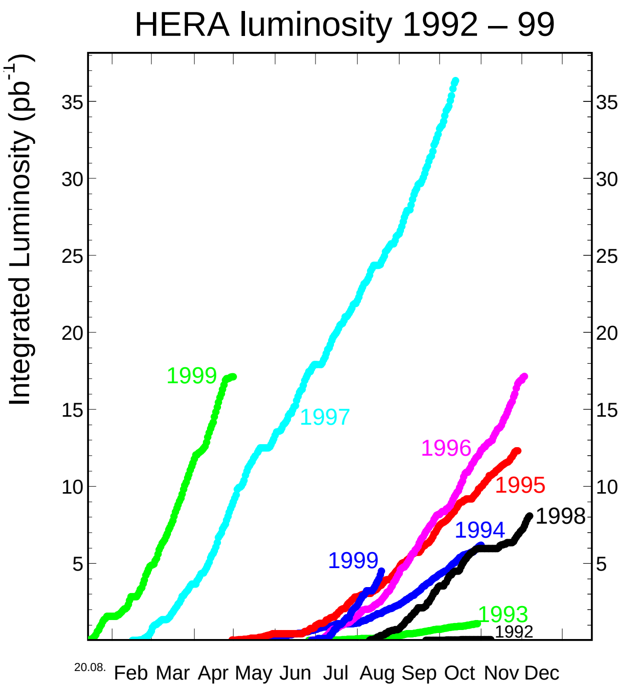

Integrated luminosity (pb−1):

	$H1$	$ZEUS$	E_p
e^+p	37	48	820 GeV
e^-p	14	13	920 GeV

Kinematic variables

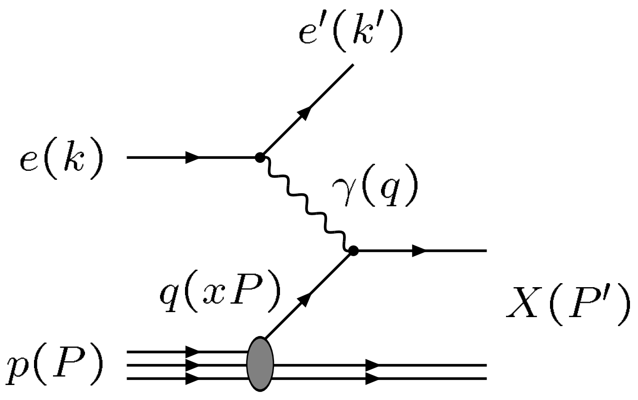

HERA 94–97 (98-99):

positrons (e^+/e^-)
$E_e = 27.5$ GeV

protons
$E_p = 820(920)$ GeV

energy in c.m.s.
$\sqrt{s} = 300(320)$ GeV

Kinematic variables:

- $Q^2 = -q^2 = -(k-k')^2 = 2E_eE'_e(1-\cos\theta)$

  negative of four-momentum transfer squared

  ($-$mass^2 of virtual photon)

  low $Q^2 \Longleftrightarrow$ low scattering angle θ

- $x = \dfrac{Q^2}{2P\cdot q} = \dfrac{Q^2}{sy}$ $\qquad 0 < x < 1$

  momentum fraction of struck parton in proton

- $y = \dfrac{P\cdot q}{P\cdot k} = 1 - \dfrac{E'_e}{2E_e}(1+\cos\theta)$ $\qquad 0 < y < 1$

  fract. energy transfer to proton in its rest frame

- $W^2 = (P+q)^2 = \dfrac{Q^2(1-x)}{x} + m_p^2$

  photon-proton center-of-mass energy

  (mass^2 of hadronic system)

HERA kinematic range

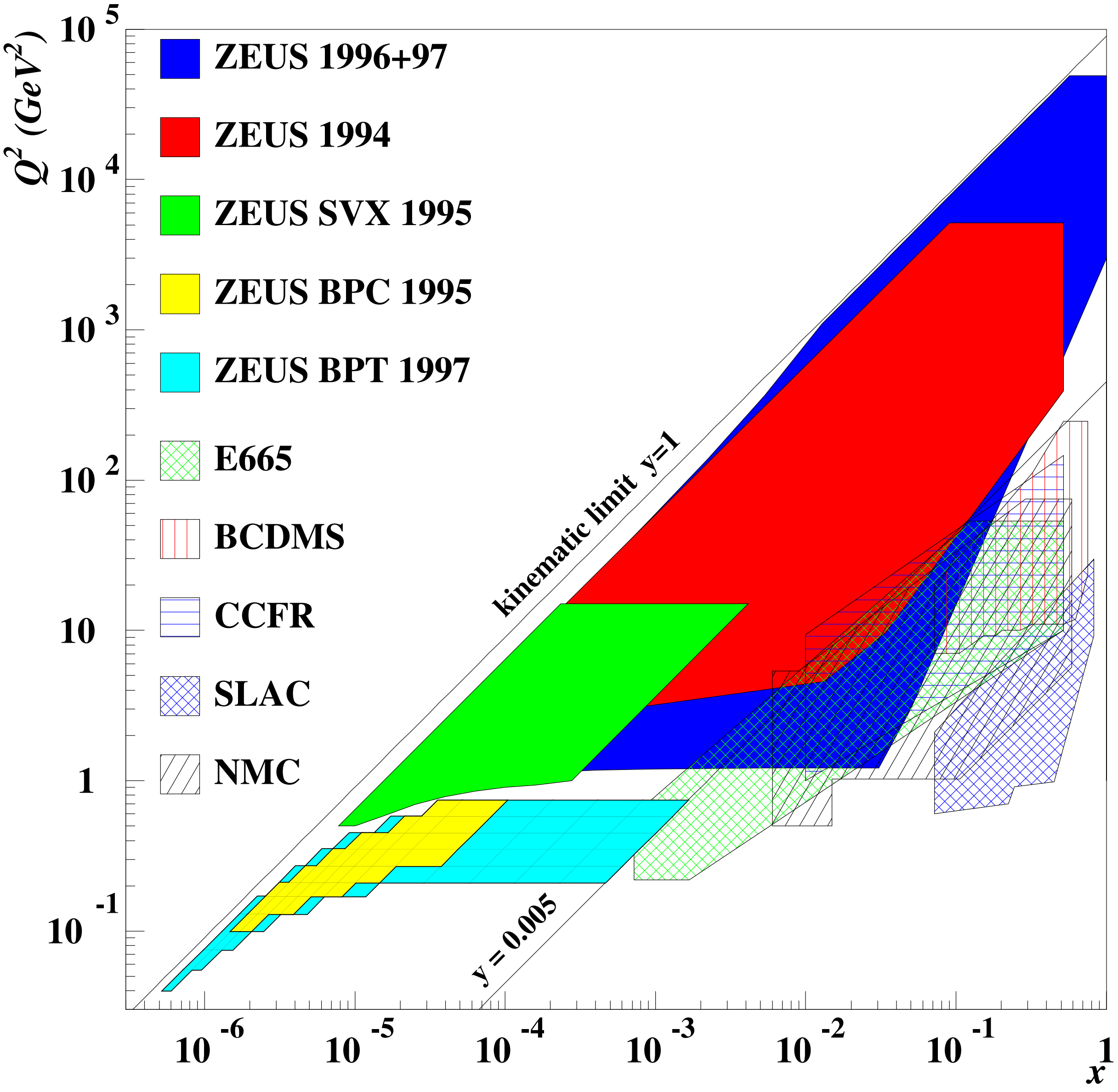

- $y \to 1$: sensitivity to F_L
- $y \to 0.005$: overlap with fixed-target experiments
- low Q^2: transition from $\gamma^* p$ to γp
- medium Q^2: tests of pQCD
- high Q^2: electroweak studies, (new physics?)

Structure functions –NC

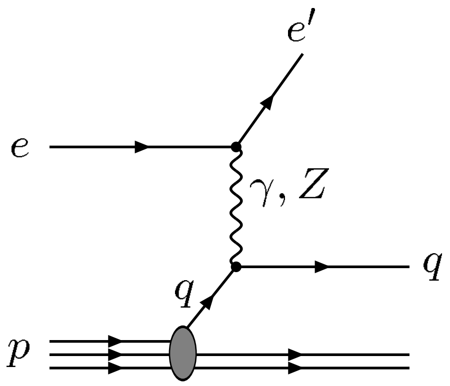

NEUTRAL CURRENT (NC)
Scattered e^+ in a detector;
e^+ balances hadronic p_T

Differential $e^{\pm}p \to e^{\pm}X$ cross section:

$$\boxed{\frac{d^2\sigma(NC)}{dx\,dQ^2} = \frac{2\pi\alpha^2}{xQ^4}\left(Y_+F_2^{NC} - y^2F_L^{NC} \mp Y_-xF_3^{NC}\right)}$$

$$\boxed{\frac{d^2\sigma^{LO}(e^+p)}{dx\,dQ^2} = \frac{2\pi\alpha^2}{xQ^4}Y_+\left(\frac{4}{9}x(u+\bar{u}) + \frac{1}{9}x(d+\bar{d})\right)}$$

- $Y_{\pm} = 1 \pm (1-y)^2 \Rightarrow$ gives helicity dependence

Structure functions of the proton:

- $F_2^{NC}(x,Q^2) = \sum_q x\,e_q^2\left[q(x,Q^2) + \bar{q}(x,Q^2)\right]$

  $+$ corrections in higher orders QCD

  $q,\ \bar{q}$: parton density functions

  $$F_2 = F_2^{\text{em}} + \left(\frac{Q^2}{Q^2+M_Z^2}\right)F_2^{\text{int}} + \left(\frac{Q^2}{Q^2+M_Z^2}\right)^2 F_2^{\text{weak}}$$

  "the" structure function of the proton
- $F_L^{NC}(x,Q^2)$

  at leading order (QPM), $F_L(x,Q^2) = 0$

  longitudinal structure function
- $xF_3^{NC}(x,Q^2)$: negligible for $Q^2 \ll M_Z^2$

  parity violating term

Structure functions – CC

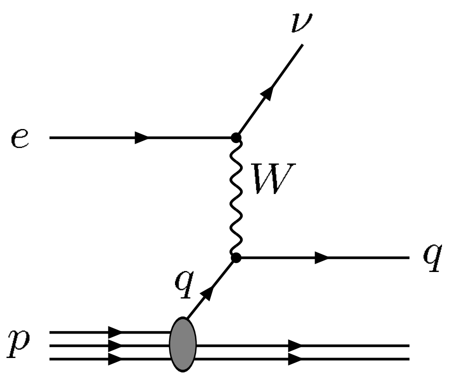

CHARGED CURRENT (CC)
Scattered ν not observed;
Only the hadronic system is measured

Differential $e^{\pm}p \to \nu X$ cross section:

$$\boxed{\frac{d^2\sigma(CC)}{dx\,dQ^2} = \frac{G_F^2}{4\pi x}\left(\frac{M_W^2}{M_W^2+Q^2}\right)^2 (Y_+F_2^{CC} - y^2F_L^{CC} \mp Y_-xF_3^{CC})}$$

$$\boxed{\frac{d^2\sigma^{LO}(e^+p)}{dx\,dQ^2} = \frac{G_F^2}{2\pi x}\left(\frac{M_W^2}{M_W^2+Q^2}\right)^2 (x\bar{u} + (1-y)^2 xd)}$$

G_F = Fermi Coupling Constant

Overview of F_2

Example: $e^+p \to e^+X$ (NC):

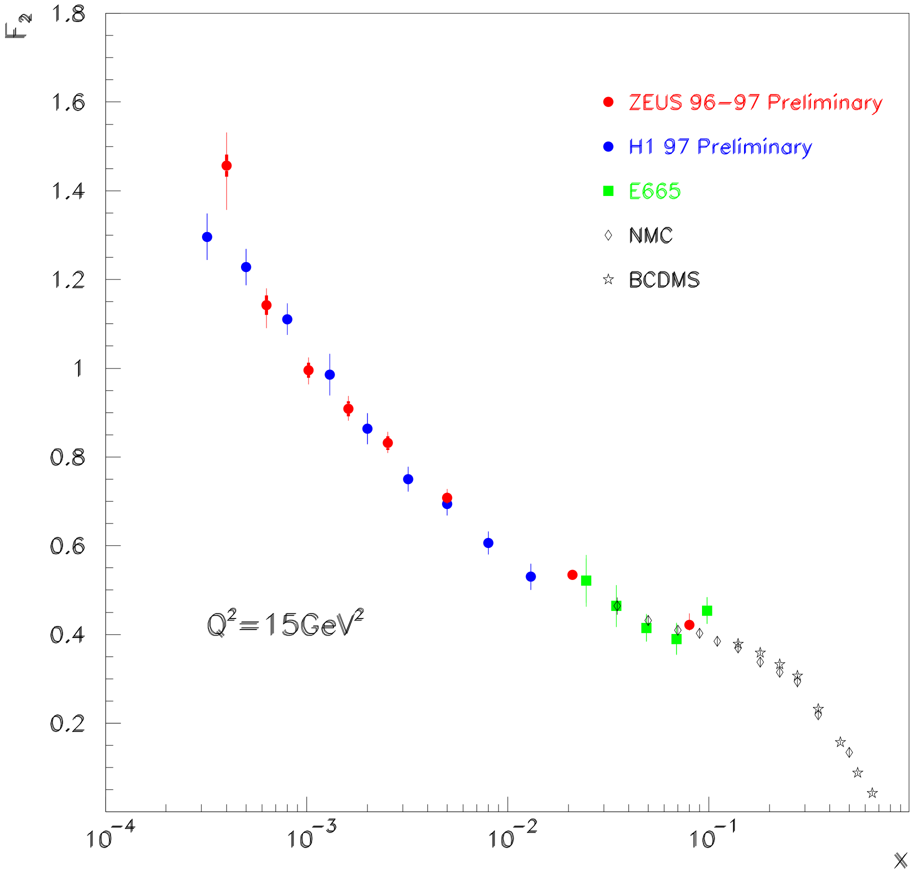

- fixed-target experiments:
  high $x \to$ valence quarks
- "first" HERA result:
  strong rise of F_2 as x decreases
  low $x \to$ sea quarks $\to$ rising gluon
- good agreement between ZEUS and H1
  and between HERA and fixed-target

NLO QCD fits assume functional forms for the quark and gluon densities and then fit to the data. The parameters of the fit are constants in the assumed functions.

Scaling violations of F_2 – NC

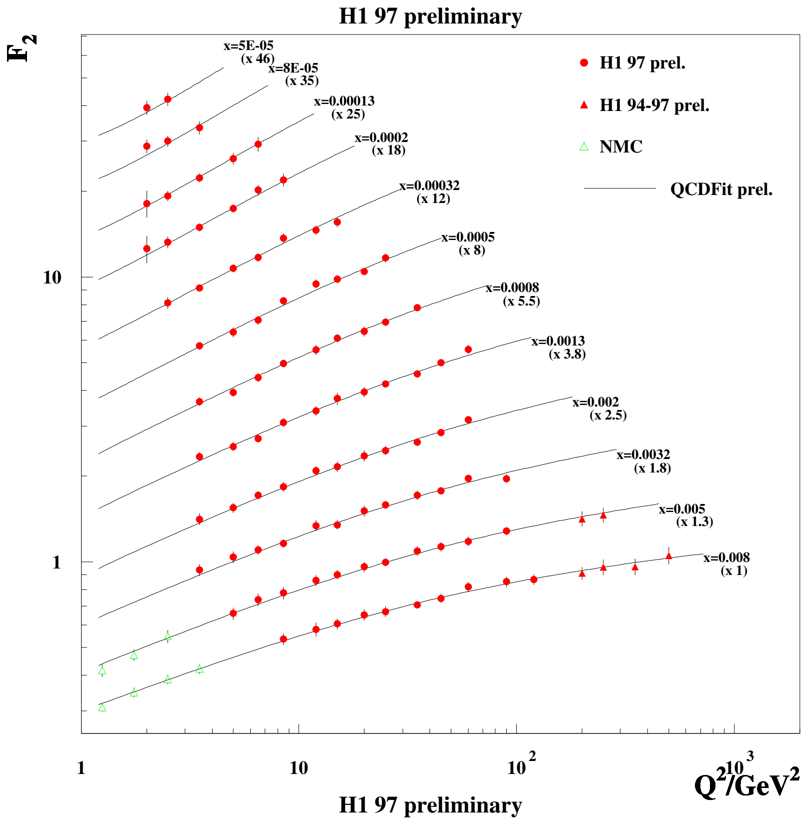

$\Leftarrow$ at small x,
F_2 rises with Q^2
scaling violations
driven by the gluon density (DGLAP):

$$\boxed{\frac{dF_2}{dlnQ^2} \sim \alpha_s P_{qg} \otimes xg}$$

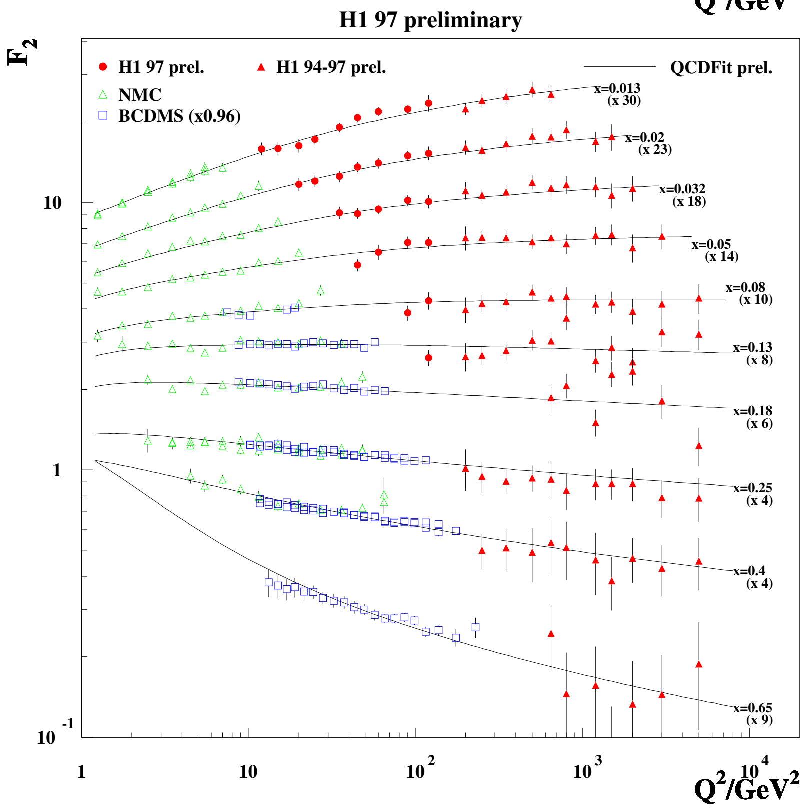

$\Leftarrow$ at $x \sim 0.1$
scale invariance
$F_2(x, Q^2) \to F_2(x)$

- NLO QCD fit describes the data over 4 orders of magnitude in both Q^2 and x

F_2 at high Q^2

Compare $e^{\pm}p$, NC and CC:

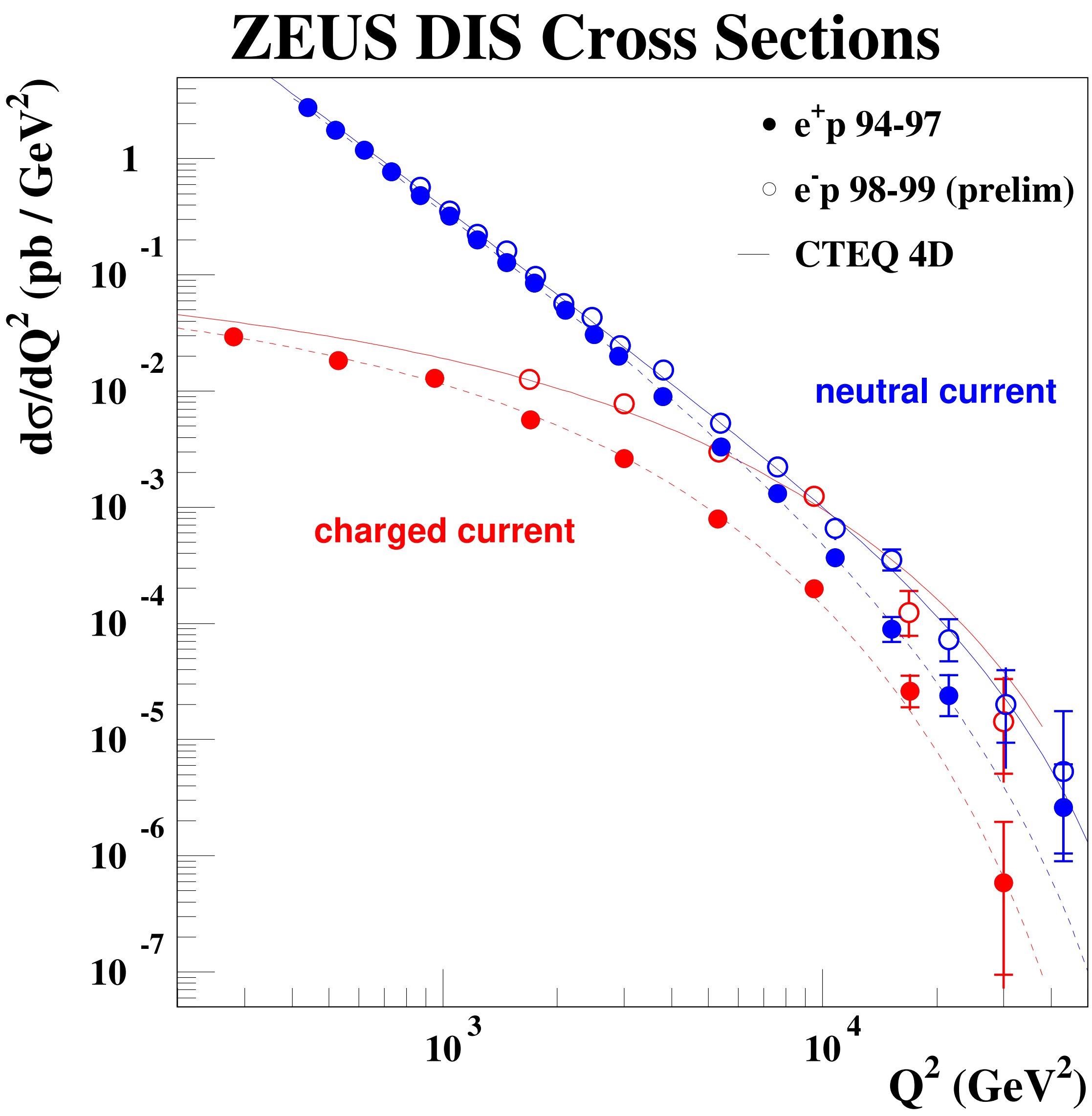

- for large Q^2, NC and CC processes have similar magnitude cross sections
- electroweak unification scale is $\sim 10^4$ GeV^2
- details of the processes depend on the quark flavors and couplings

F_2 at high Q^2 – NC (1)

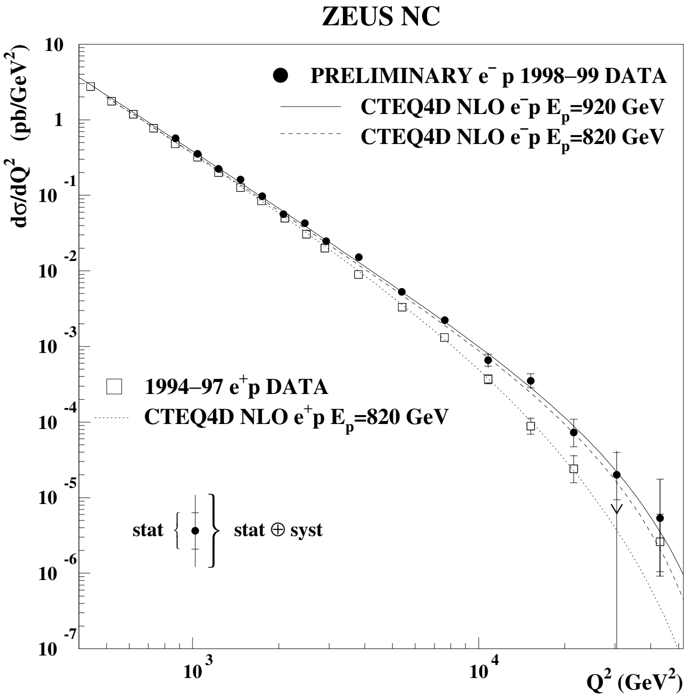

The NLO QCD fits to lower Q^2 data describe the high Q^2 data well

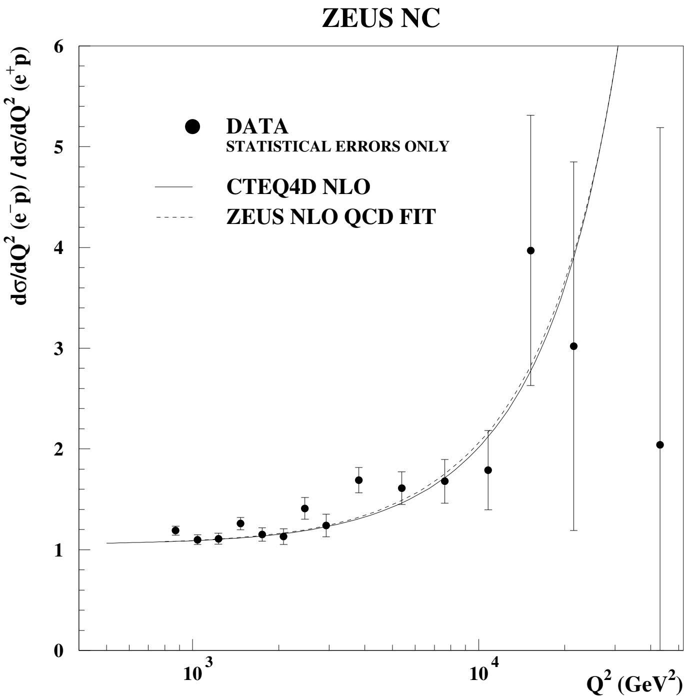

Ratio $\frac{e^-p}{e^+p}$ for NC:

At high Q^2,
$e^-p > e^+p$
$\gamma - Z$ interference

- excellent agreement with the Standard Model (over 6 orders of magnitude in cross section)

F_2 at high Q^2 – NC (2)

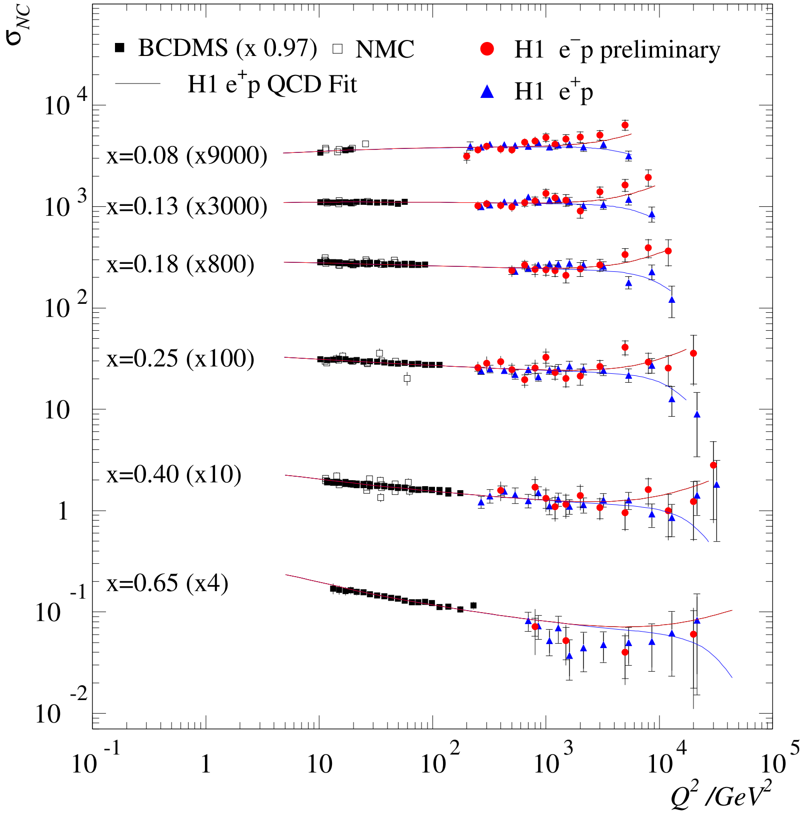

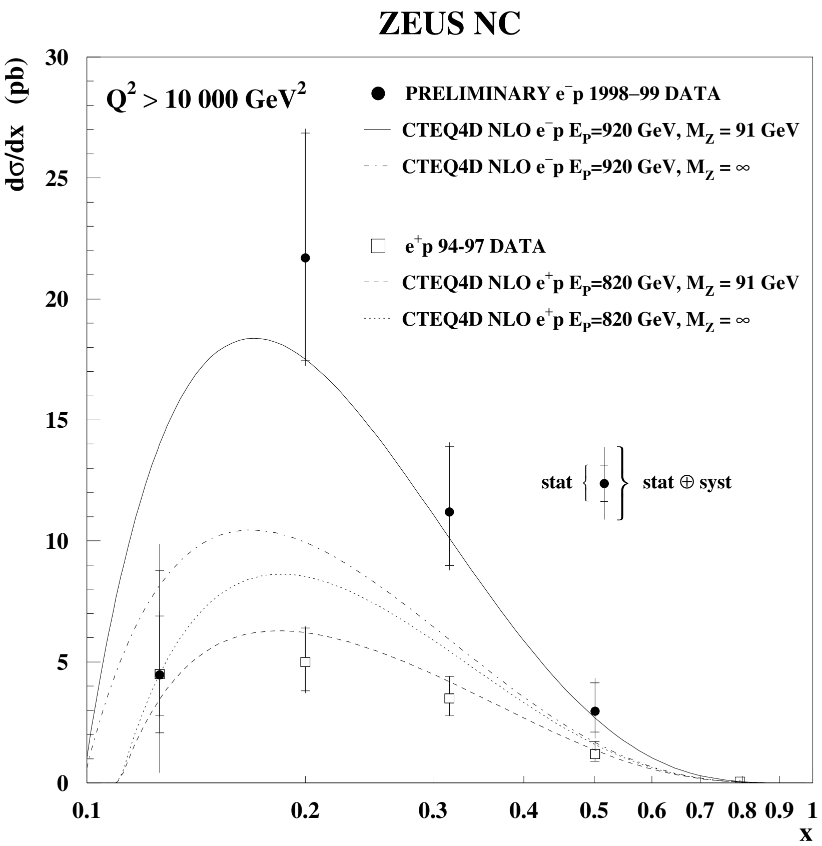

- Difference between e^+p and $e^-p \rightarrow$ evidence of $\gamma - Z$ interference
- Negative interference in e^+p, positive in e^-p
- Evidence for Z exchange in the space-like region of DIS

F_2 at high Q^2 – CC (1)

For e^+p:

$$\boxed{\tilde{\sigma} = \frac{2\pi x}{G_F^2}\frac{(Q^2 + M_W^2)^2}{M_W^4}\frac{d^2\sigma^{CC}}{dxdQ^2} = x[\bar{u} + (1-y)^2 d]}$$

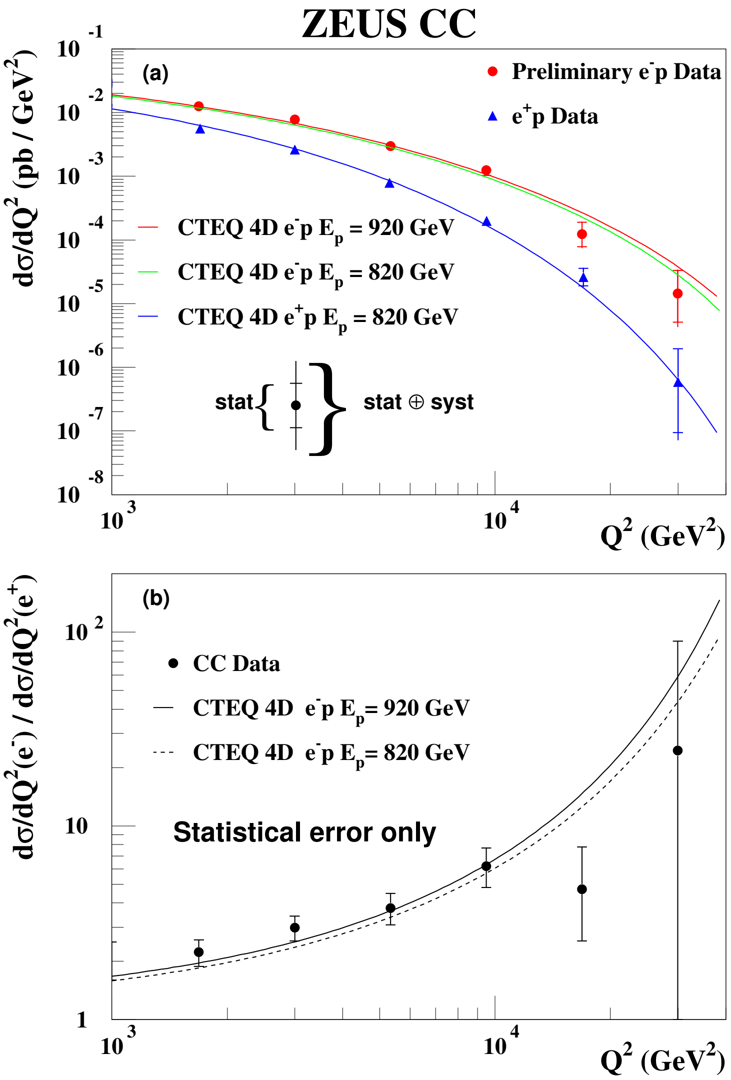

$e^- \sim xu$

$e^+ \sim (1-y)^2 xd$

Ratio $\dfrac{e^-p}{e^+p}$ for CC

$\sim$ 10, at high Q^2

- excellent agreement with SM and CTEQ4D pdf
- determine the mass of the W-boson from the propagator shape:

$$\boxed{\frac{d\sigma^{CC}}{dQ^2} \propto G_F^2 \cdot \left[\frac{M_W^2}{Q^2 + M_W^2}\right]^2}$$

F_2 at high Q^2 – CC (2)

Effects of the W propagator

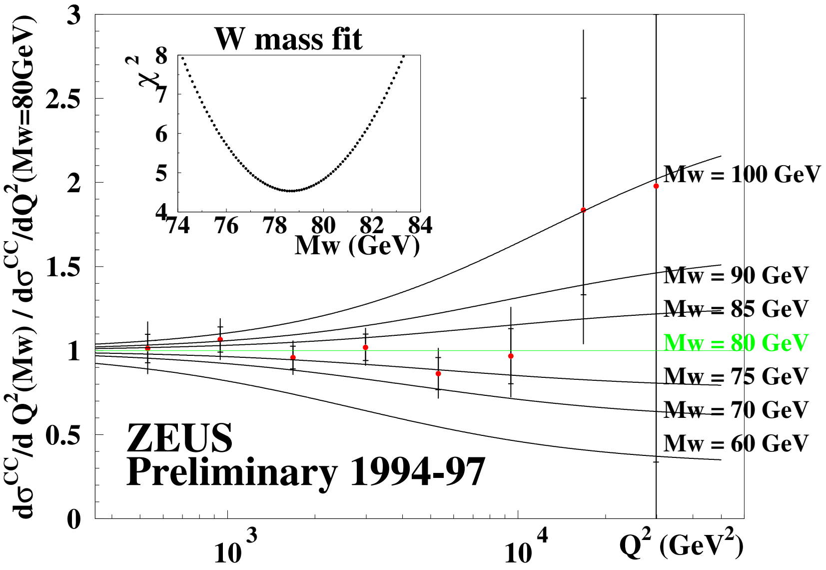

Fix G_F, fit for M_W:

ZEUS: $M_W = 81.4^{+2.7}_{-2.6} \pm 2.0^{+3.3}_{-3.0}(pdf)$GeV
H1: $M_W = 80.9 \pm 3.3 \pm 1.7 \pm 3.7(pdf)$GeV

$M_W = 80.41 \pm 0.10$ (PDG 98)

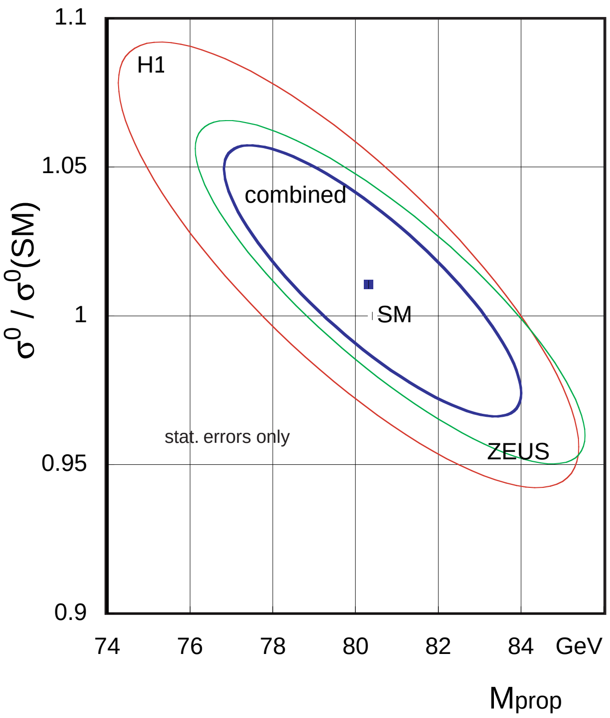

$$\frac{d\sigma}{dQ^2} = \sigma^0 \left[\frac{M^2_{prop}}{M^2_{prop} + Q^2}\right]^2 \Phi_W$$

Φ_W = quark densities

- Space-like measurement of the W-boson!

F_2 at high Q^2 – CC (3)

Quark Content in e^+p

Reduced cross section $\Rightarrow$ propagator effects diminish, pdf's are more visible

$$\boxed{\tilde{\sigma} = \frac{2\pi x}{G_F^2}\frac{(Q^2+M_W^2)^2}{M_W^4}\frac{d^2\sigma^{CC}}{dxdQ^2} = x[(\bar{u}+\bar{c}) + (1-y)^2(d+s)]}$$

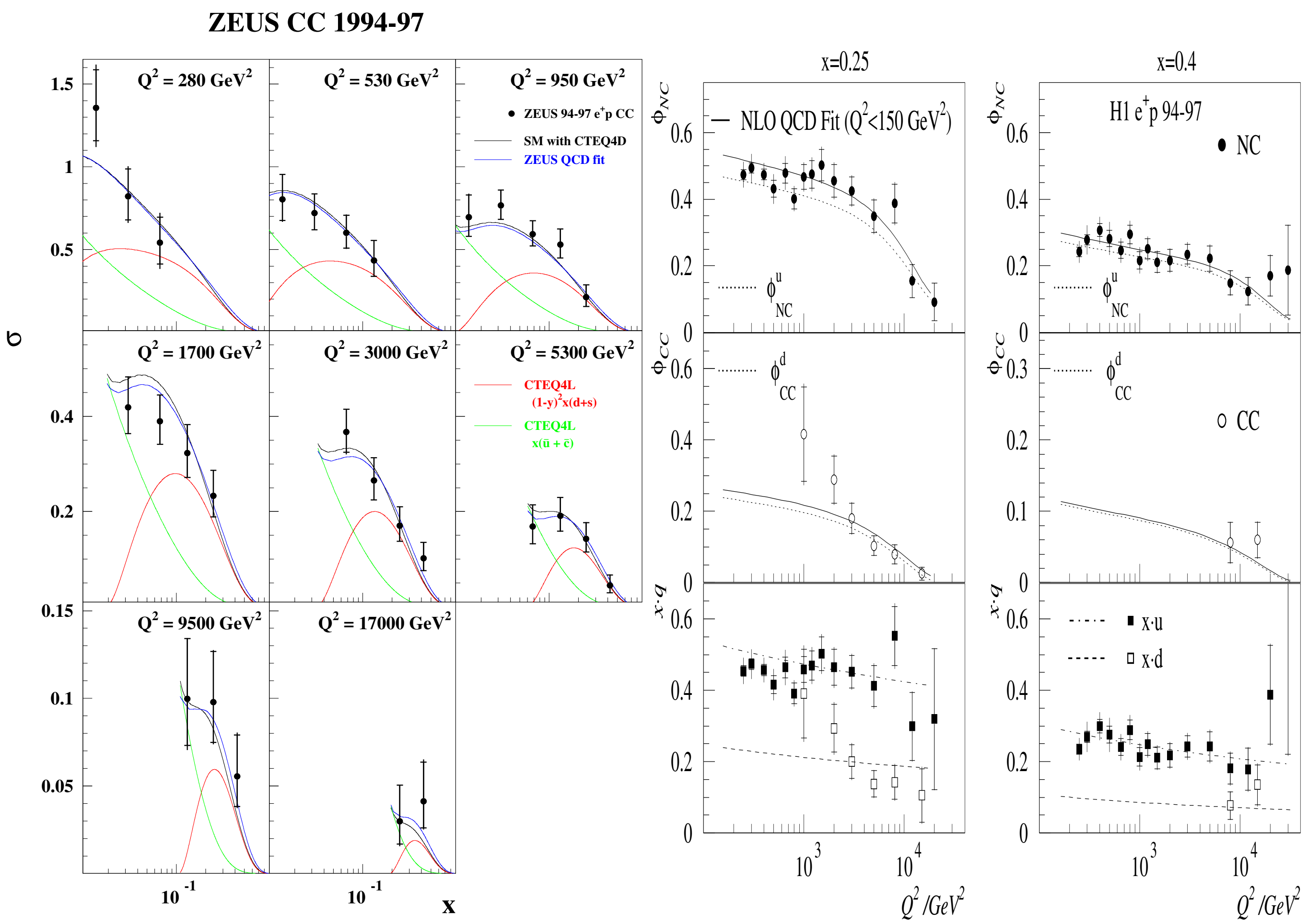

- at high Q^2, $\tilde{\sigma}$ dominated by d-quark
- good agreement with the SM and pdf from low Q^2
- the data can be used to constrain particular parton flavors for the proton structure

F_2 at medium Q^2 – NC

$$\sigma_r = \frac{d^2\sigma(ep \to eX)}{dx\, dQ^2} \cdot \frac{xQ^4}{2\pi\alpha^2} = F_2 - \frac{y^2}{Y_+} F_L$$

- for $y^2 F_L \ll Y_+ F_2$:

$$\sigma_r \approx F_2$$

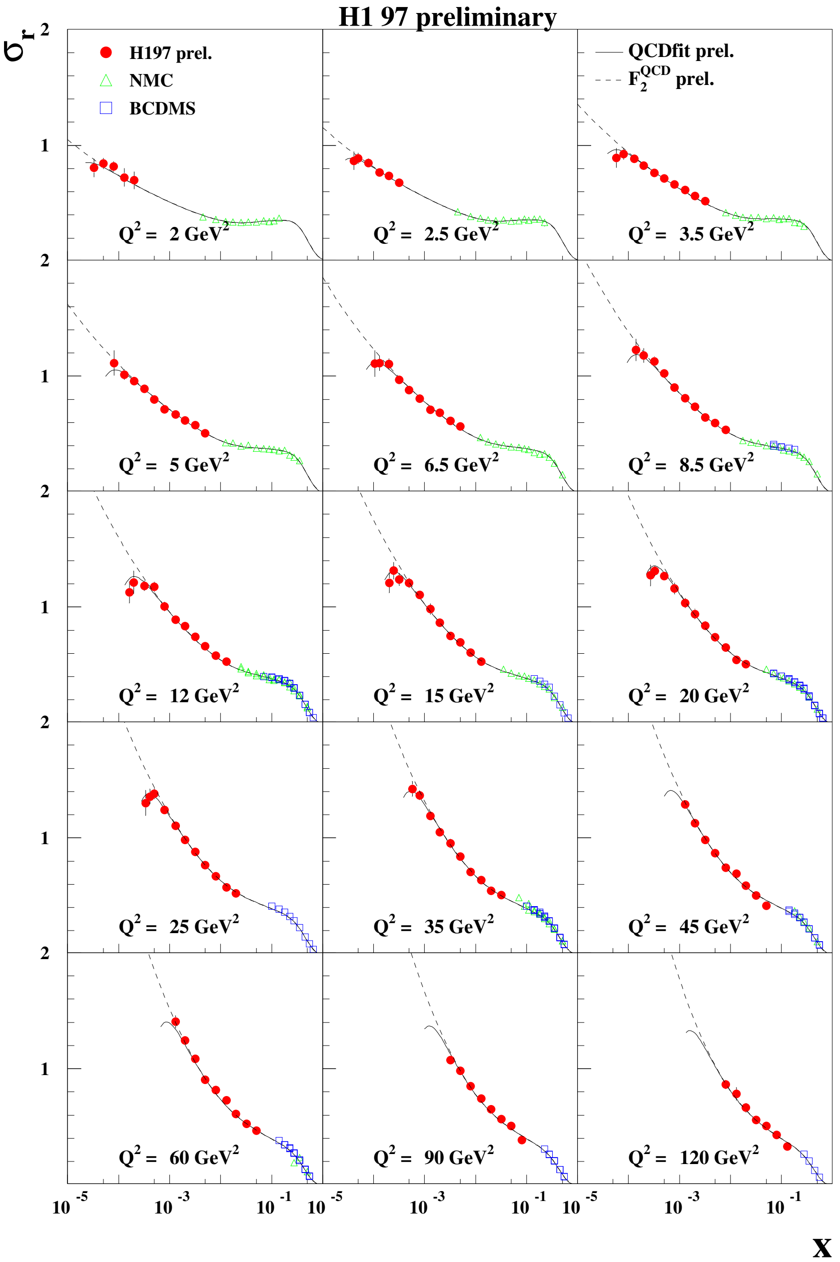

- F_2 steepens with Q^2: $\rightarrow$ increase of the gluon
- at high y (low x): $\sigma_r \neq F_2 \rightarrow$ sensitive to F_L
- for $y \rightarrow 1$:

$$F_L \approx F_2 - \sigma_r$$

Extraction of F_L

Direct F_L measurement needs variation of beam energies

Indirect extraction of F_L:

- make a DGLAP fit to F_2 in a region where the contribution from F_L is negligible (y small)
- extrapolate F_2 from fit to higher y ($y \approx 0.7 - 0.8$)
- extract $F_L = \frac{Y_+}{y^2}\left(F_2^{\text{fit}} - \sigma_r^{\text{measured}}\right)$

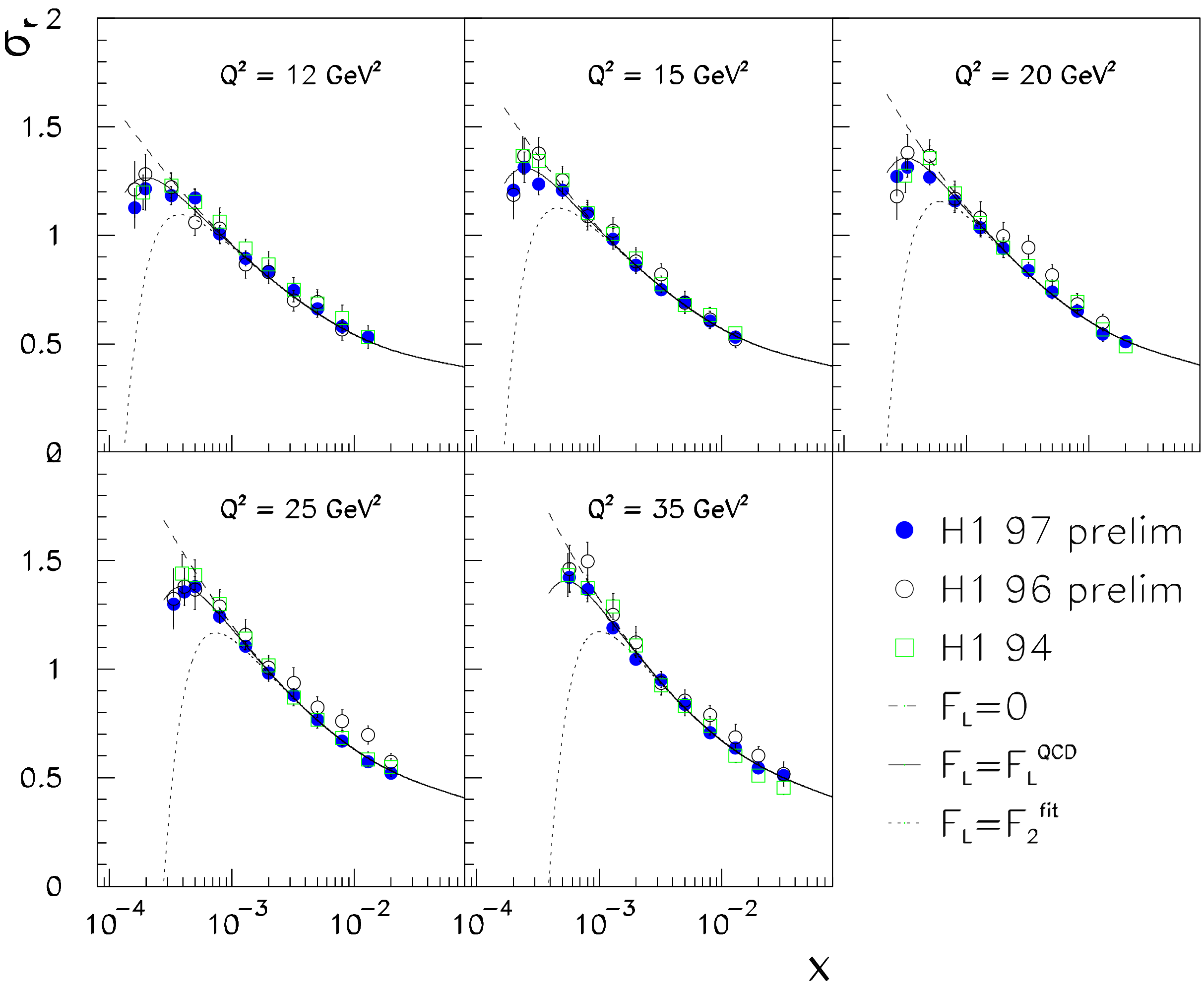

Data are consistent with an $F_L = F_L^{QCD}$

F_2 at low Q^2

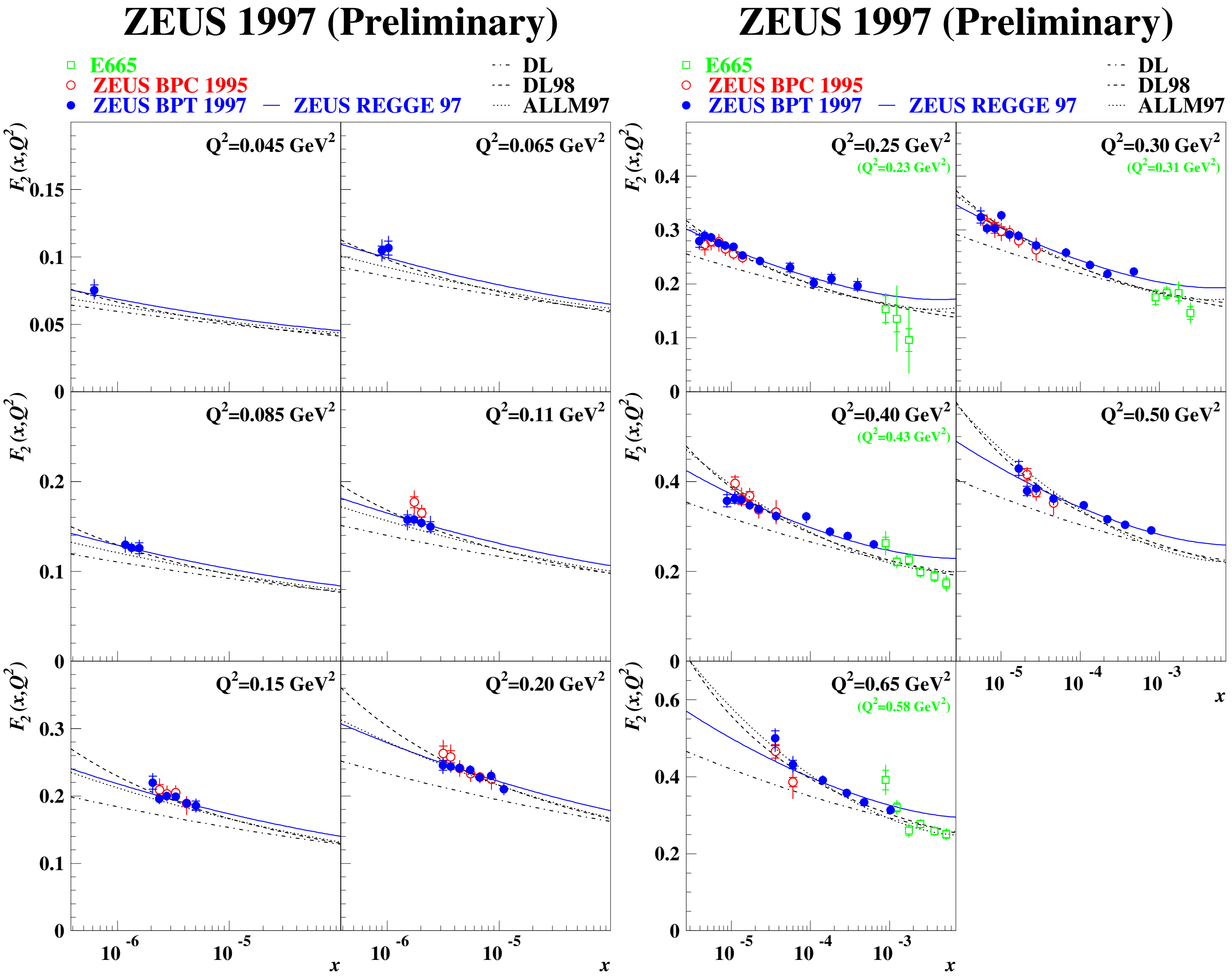

- F_2 rises even at the lowest Q^2
- F_2 is small ($F_2 \propto Q^2$ for $Q^2 \to 0$)

Factorization in γ^* flux and $\gamma^* p$ cross section:

$$\boxed{\frac{d^2\sigma(ep \to eX)}{dy\, dQ^2} = \Gamma \cdot \left(\sigma_T^{\gamma^* p} + \epsilon\, \sigma_L^{\gamma^* p}\right)}$$

- $\Gamma = \alpha Y_+ / 2\pi y Q^2$: virtual photon flux
- $\epsilon = 2(1-y)/Y_+$: photon polarization
- at low x:

$$\sigma_{\text{tot}}^{\gamma^* p} = \sigma_T^{\gamma^* p} + \sigma_L^{\gamma^* p} \approx \frac{4\pi^2\alpha}{Q^2} F_2$$

W^2 dependence of $\sigma_{\text{tot}}^{\gamma^* p}$

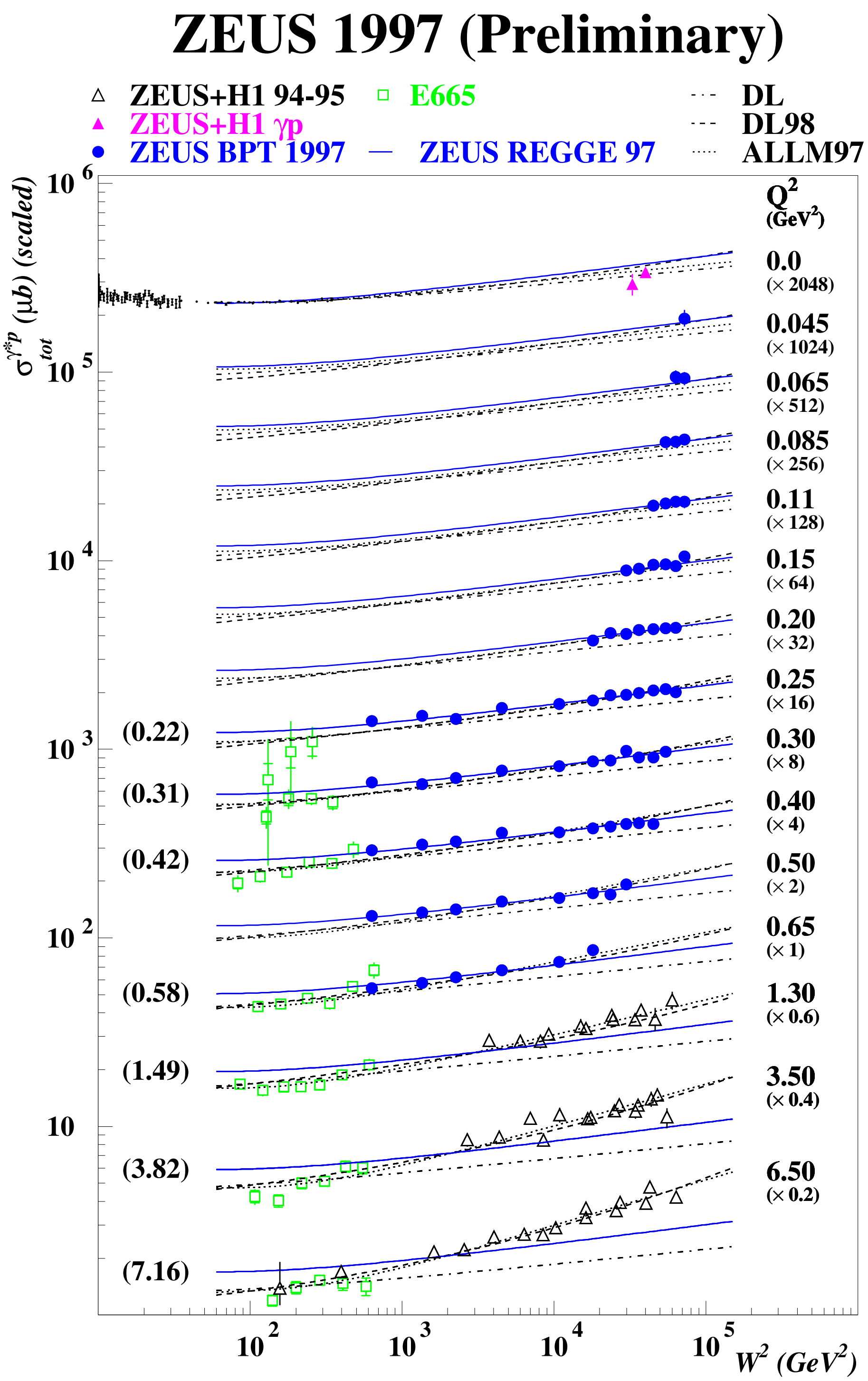

- rise of: F_2 at low x $\Longleftrightarrow$ $\sigma_{\text{tot}}^{\gamma^* p}$ at high $W^2 \sim \frac{Q^2}{x}$
- low Q^2: $\sigma_{\text{tot}}^{\gamma^* p} \propto (W^2)^{0.11}$
- high Q^2: $\sigma_{\text{tot}}^{\gamma^* p} \propto (W^2)^{0.2-0.4}$

The rise of F_2

Measure of the rise of F_2:

- $\lambda_{\text{eff}} = \dfrac{d \log F_2}{d \log(1/x)}$
- λ_{eff} constant: $F_2 \propto x^{-\lambda_{\text{eff}}}$ or $\sigma_{\text{tot}}^{\gamma^* p} \propto (W^2)^{\lambda_{\text{eff}}}$
  $\lambda_{\text{eff}} \approx \alpha_{\mathbb{P}} - 1$ (if Pomeron exchange dominates)
- extract λ_{eff} from fit to the data ($x < 0.01$)
- Note: averaging over Q^2-dependent x range

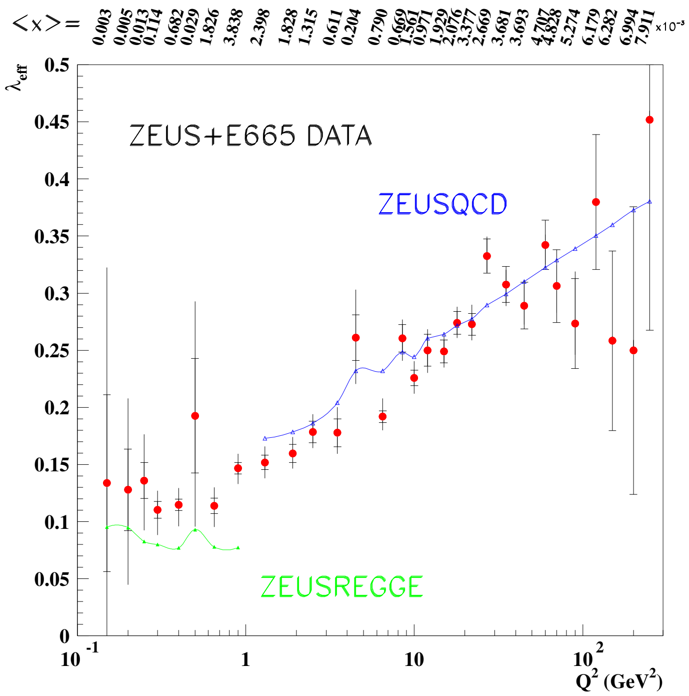

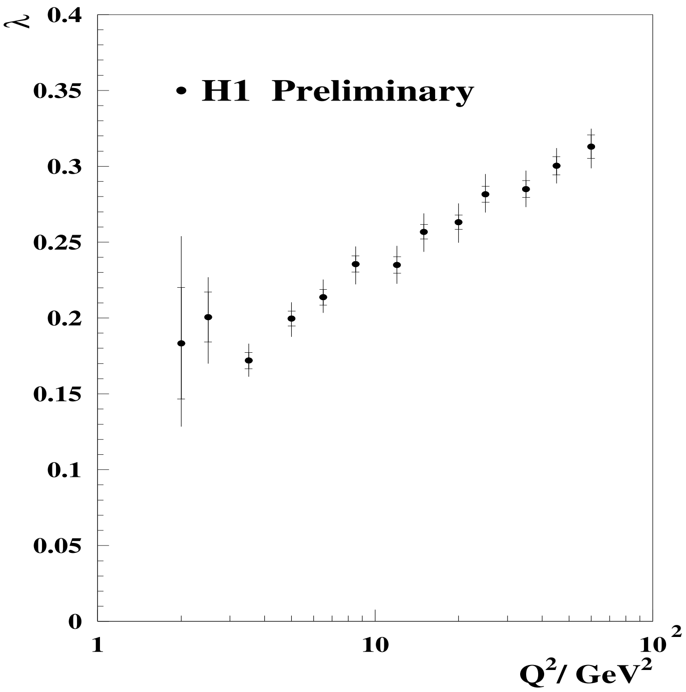

Result:

- lowest Q^2: constant and larger than 0.08 (soft Pomeron)
- higher Q^2: $\approx$ logarithmic rise with Q^2

Q^2-dependence of $\sigma_{\text{tot}}^{\gamma^* p}$

- Simplified Q^2 dependence of $\sigma_{\text{tot}}^{\gamma^* p}$ à la GVDM:

$$\sigma_{\text{tot}}^{\gamma^* p}(W^2, Q^2) = \left(\frac{m_0^2}{m_0^2 + Q^2}\right) \sigma_{\text{tot}}^{\gamma p}(W^2)$$

- Extract values of $\sigma_{\text{tot}}^{\gamma p}(W^2)$ from fit to the data
  $m_0 \approx \rho$ mass

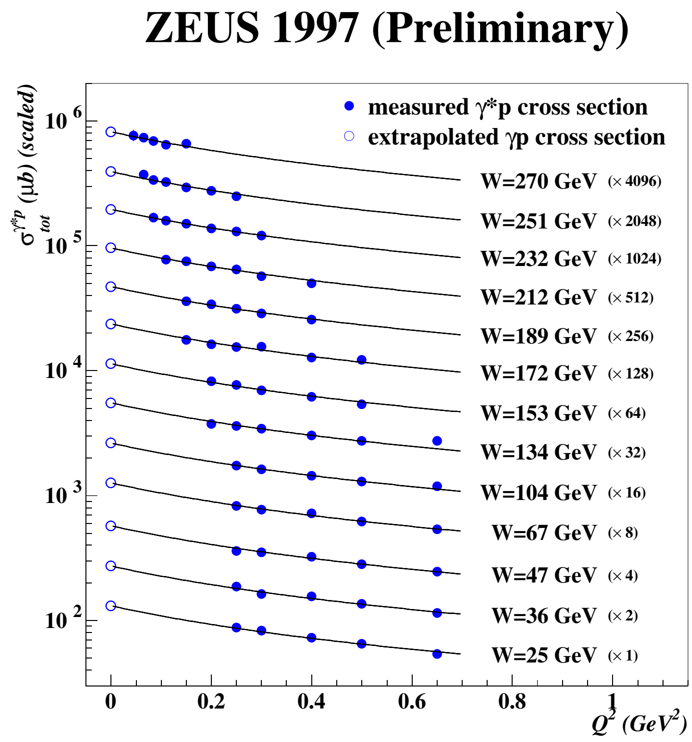

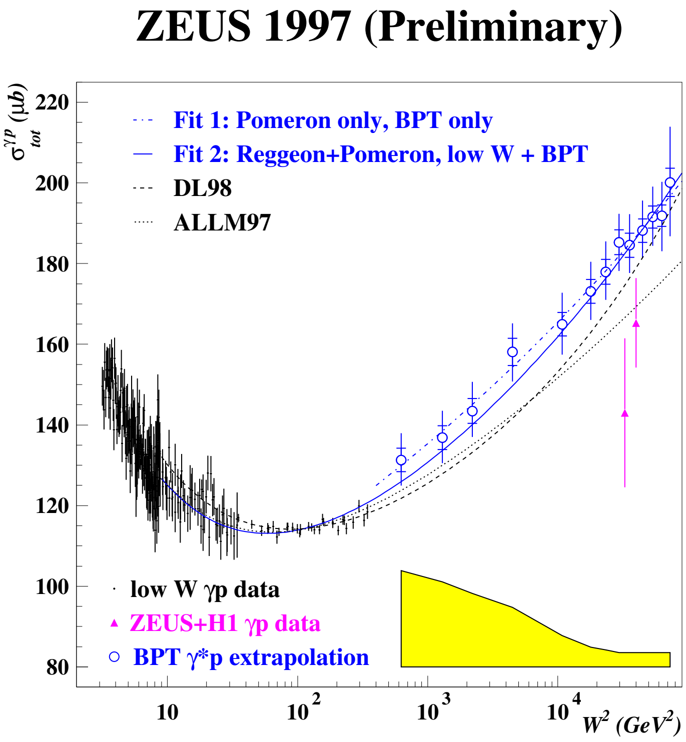

- yellow band: estimated model-dependence

- blue line: $\sigma_{\text{tot}}^{\gamma p}(W^2) = A_{\mathbb{R}} W^{2(\alpha_{\mathbb{R}}-1)} + A_{\mathbb{P}} W^{2(\alpha_{\mathbb{P}}-1)}$
  $\alpha_{\mathbb{P}}$ compatible with soft Pomeron

Inclusive diffraction (1)

Diffractive states have the same quantum numbers as the initial state $\Rightarrow$ vacuum qu. no. exchanged in the t-channel $\Rightarrow$ Pomeron ($\mathbb{P}$)

Inclusive diffractive at HERA corresponds to the diffractive excitation of a virtual γ:

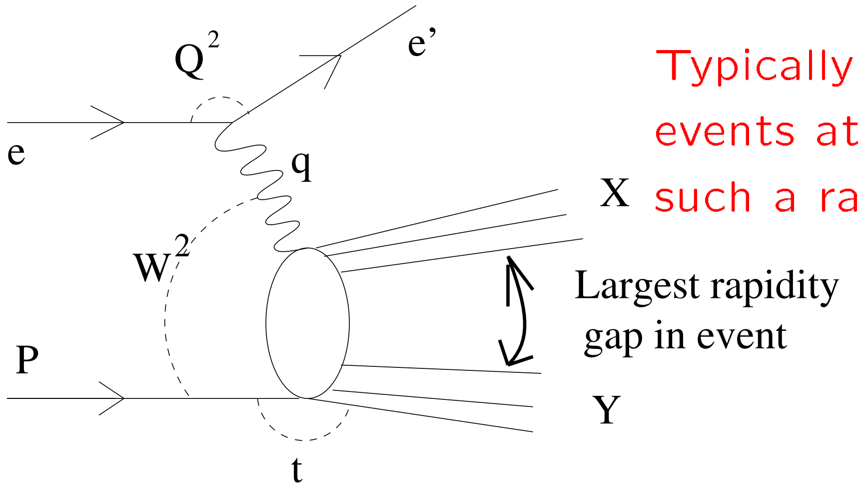

Typically $\sim$ 10% DIS events at HERA have such a rapidity gap

- the variables, in addition to Q^2, x and W, are
- $t = (p - p')^2$,
- $x_{\mathbb{P}} = \frac{q\cdot(p-p')}{q.p} \approx \frac{M_X^2+Q^2-t}{W^2+Q^2+M_p^2}$, the fraction of the proton beam momentum carried by the $\mathbb{P}$,
- $\beta = \frac{x}{x_{\mathbb{P}}} = \frac{Q^2}{2q\cdot(p-p')} \approx \frac{Q^2}{M_X^2+Q^2-t}$, the fraction of the $\mathbb{P}$ momentum carried by the struck quark.
- Define $\frac{d^4\sigma}{d\beta dQ^2 dx_{\mathbb{P}} dt} = \frac{4\pi\alpha_{em}^2}{\beta Q^4}[1 - y + \frac{y^2}{2}]F_2^{D(4)}(\beta, Q^2, x_{\mathbb{P}}, t)$
- Factorization and integration over t: $F_2^{D(3)}(\beta, Q^2, x_{\mathbb{P}}) = f_{\mathbb{P}/p}(x_{\mathbb{P}}) \cdot F_2^{\mathbb{P}}(\beta, Q^2)$
- Three methods are used to select diffractive events: M_X, leading proton spectrometer (roman pots) and a large Rapidity Gap in the forward (proton) direction.

Inclusive diffraction (2)

The original H1 NLO diffractive fits were based on the 1994 measurements:

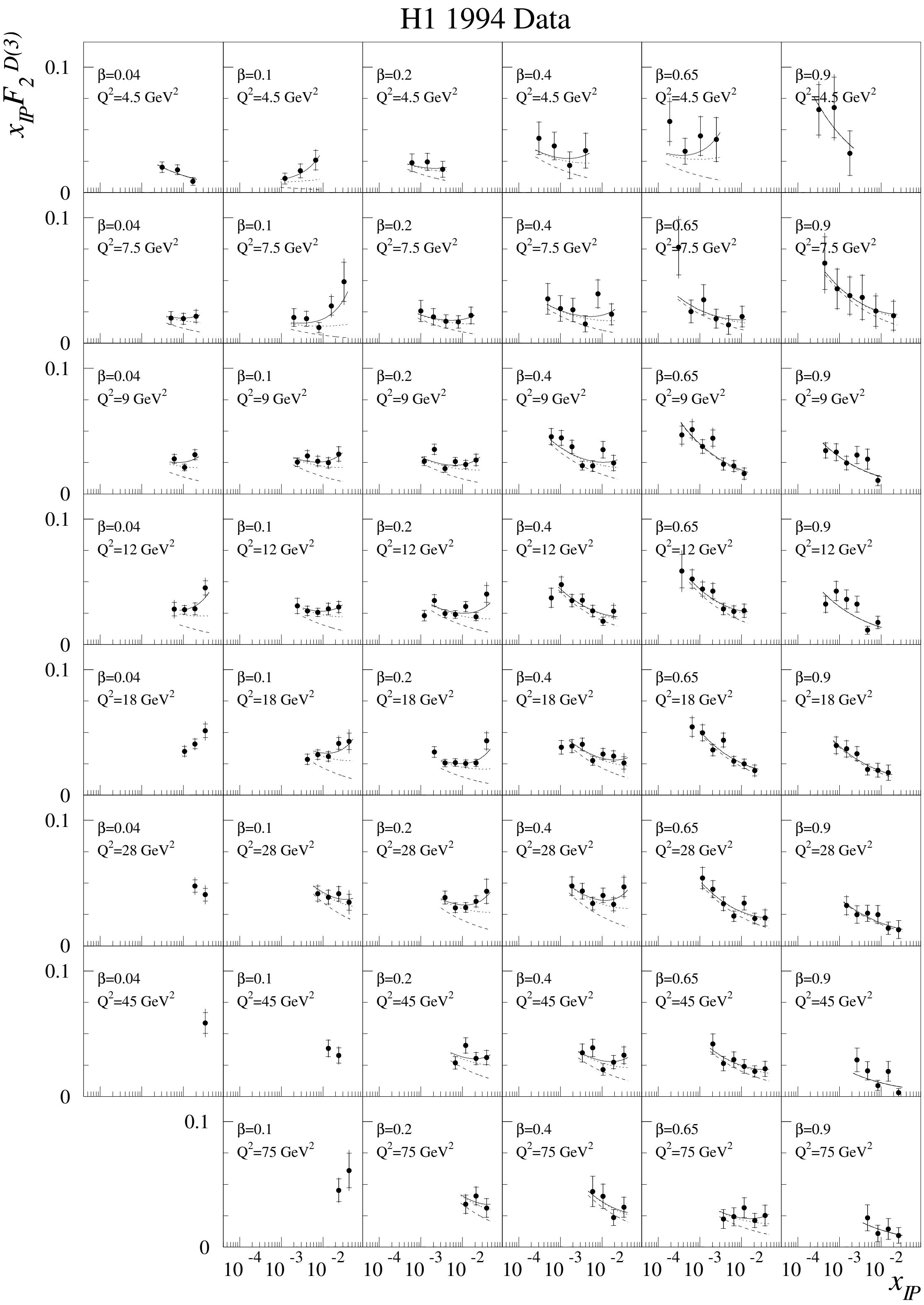

- These fits yield a large gluon component:

Inclusive diffraction (3): high Q^2

The resulting Pomeron structure (1994 data):

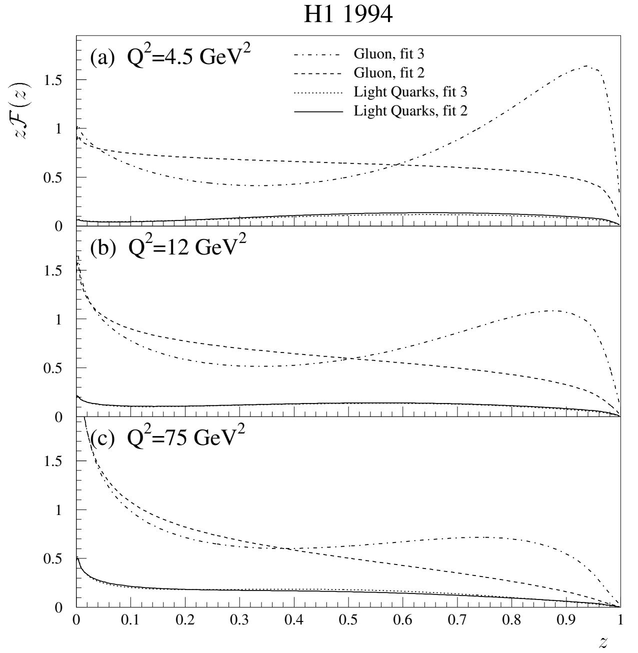

Dominant gluon $\Rightarrow$ scaling violations at large β

Scaling violations in diffract. F_2 (at $x_{\mathbb{P}} = 0.005$):

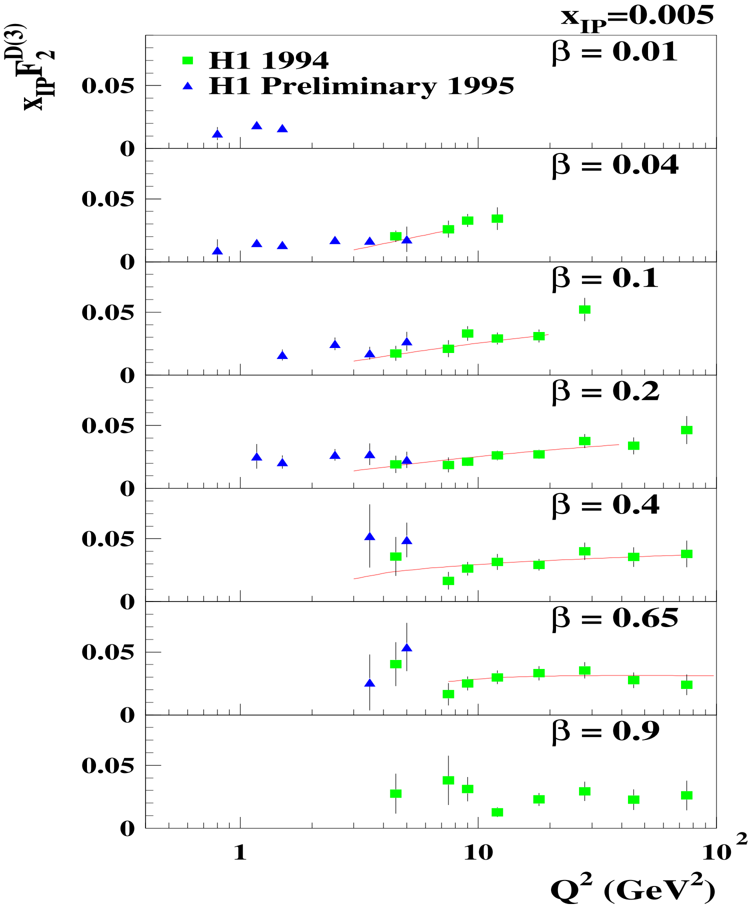

Since: scaling violations persist up to $\beta \sim 0.4$ (different from F_2), DGLAP evolution requires gluons at larger β

Vector Meson Production

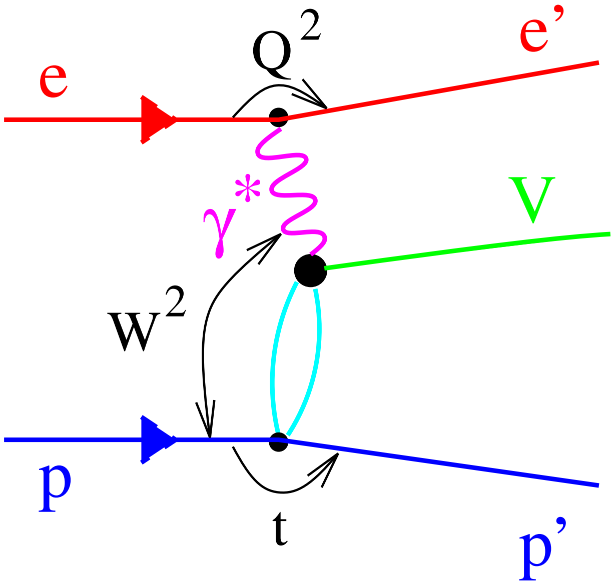

Vector meson production has proven to be an interesting testing ground for comparisons between data and pQCD models and studies of the transition from soft (non-perturbative) to hard (perturbative) scattering:

- the variables are: Q^2, M_V^2 and t (with W) and these scales can be varied in a single experiment
- the energy dependence of the cross section:

$$\boxed{\sigma = a \cdot W^\delta}$$

- ratios of the ϕ, ω and J/ψ to ρ^0 as functions of Q^2 and t. From γq coupling, one expects, SU(4):

$$\boxed{\rho^0 : \omega : \phi : J/\psi = 9 : 1 : 2 : 8}$$

$$\boxed{\rho^0 : \omega : \phi : J/\psi = 9 : (1 * 0.8) : (2 * 1.0) : (8 * 1.9)}$$

Vector Mesons (1): $Q^2 \sim 0$

Cross sections vs W ($\alpha_{\mathbb{P}}(0) = 1.08$, $\sigma_{tot} \sim W^{0.16}$):

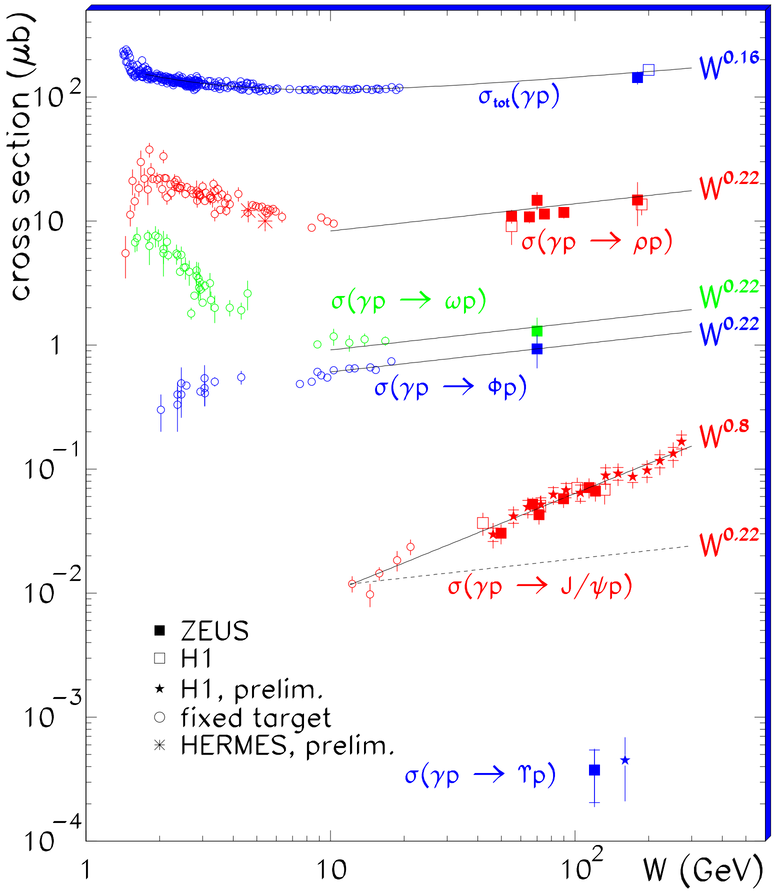

(For $\sigma_V \sim W^{0.24}$)

For ρ^0, ω, ϕ:
$\sigma \sim W^{0.22}$

$\sigma \sim W^{0.8}$
for J/ψ

J/ψ photoproduction has a steeper energy dependence than ρ^0, ω and ϕ

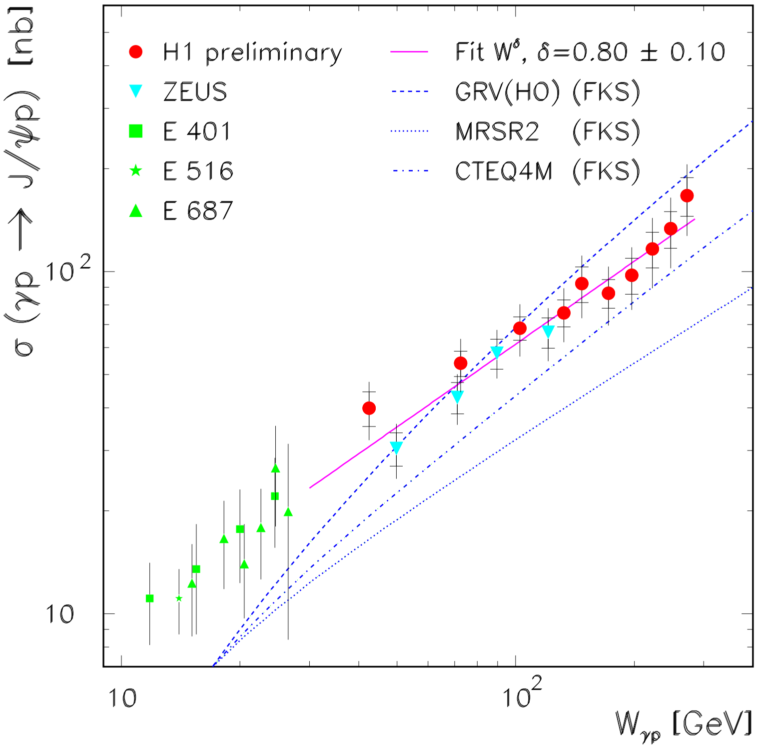

$\sigma_{pQCD} \sim |xg(x, Q^2)|^2$

$xg(x, Q^2)$ is the proton gluon density – hence a common source of the rise of F_2 and $\sigma(J/\psi)$

Vector Mesons (2) $Q^2 > 2$ GeV^2:

Study ρ^0 and J/ψ cross sections vs W:

- ρ^0
- J/ψ

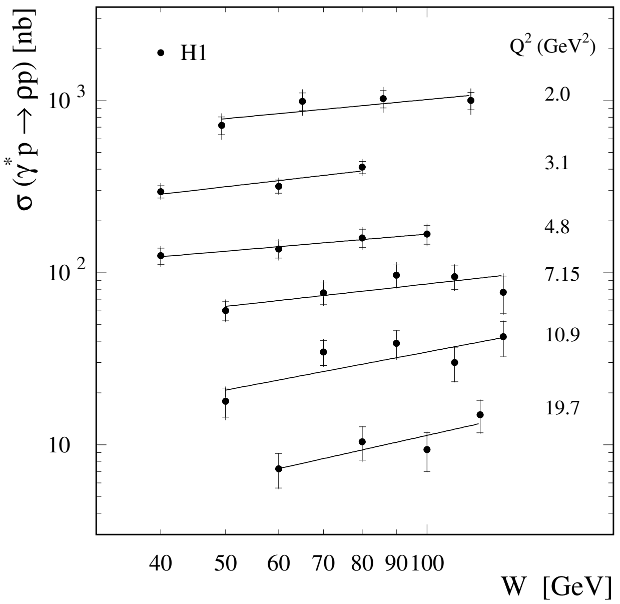

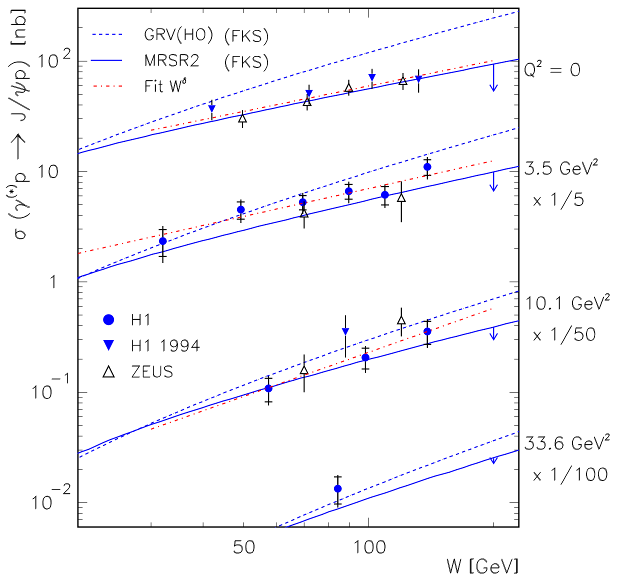

- Parameterize $\sigma \sim W^{\delta}$:

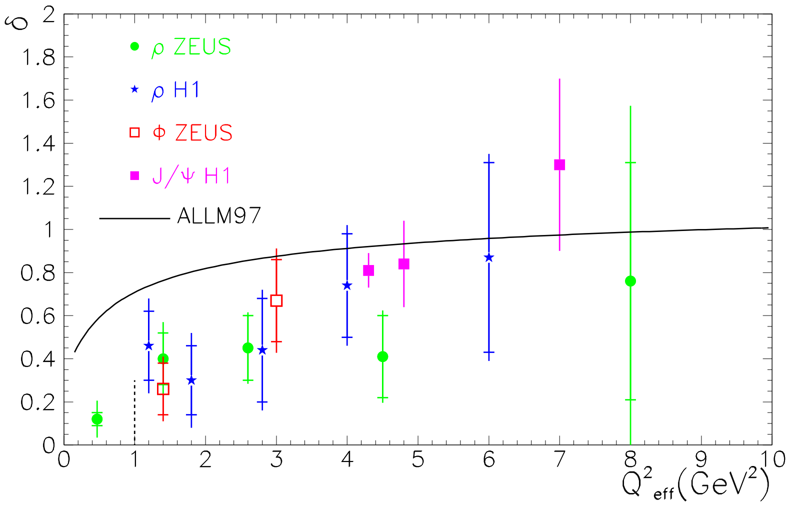

- with $Q^2_{eff} \approx \frac{<b^2_{\sigma L}>}{<b^2_{\rho T}>} Q^2$ from FKS – transverse sizes
- δ increases with the increasing scale of the process – may flatten at high Q^2_{eff}?

Vector Mesons (3) Ratios

Ratios vs. Q^2:

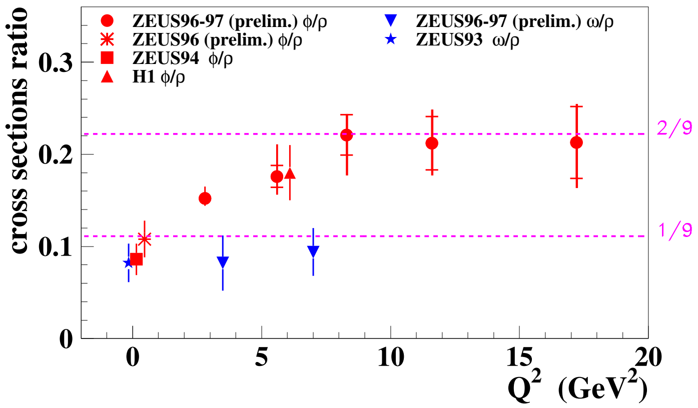

$\frac{\phi}{\rho^0}$

$\frac{\omega}{\rho^0}$

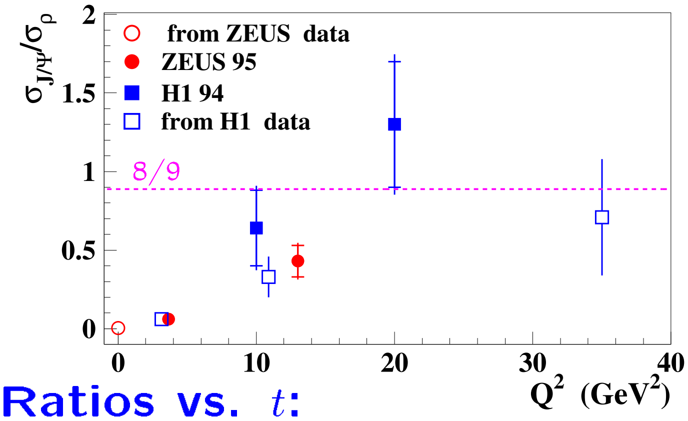

$\frac{J/\psi}{\rho^0}$

Ratios vs. t:

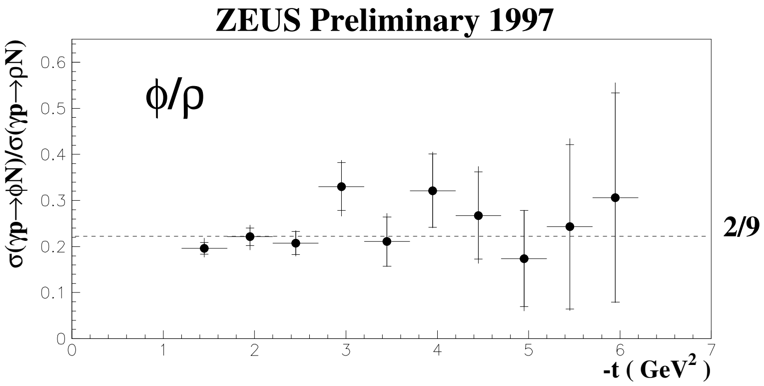

$\frac{\phi}{\rho^0}$

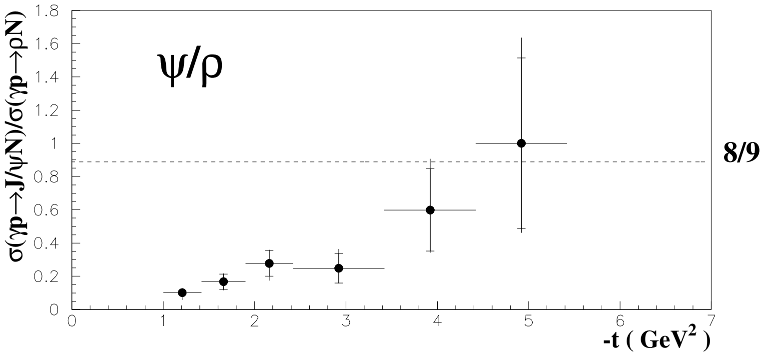

$\frac{J/\psi}{\rho^0}$

- Conclusions: flavor independence is broken at small Q^2, t, but is approached as Q^2 or t increases

Measurement of F_2^c

Semi-inclusive structure function measurement:

- require charm in the hadronic final state

$$\boxed{\frac{d^2\sigma(ep \to ec\bar{c}X)}{dy\,dQ^2} = \frac{2\pi\alpha^2}{yQ^4}\left(Y_+F_2^c - y^2F_L^c\right)}$$

- Charm is generated predominantly by boson-gluon fusion $\gamma g \to c\bar{c}$ (BGF):

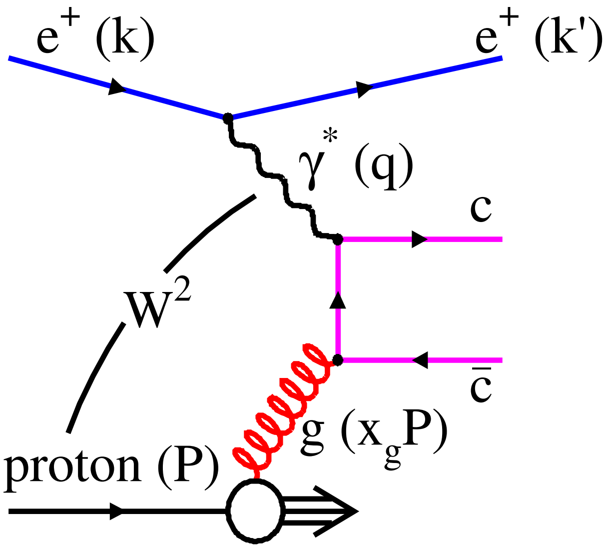

- Measure F_2^c from events with tagged charm

  e.g. $D^{*\pm} \to D^0\pi^{\pm}_{\text{slow}}$
  $\hookrightarrow K\pi$ or $K3\pi$

- neglect F_L^c ($< 1\%$)

Events with tagged charm

• $D \to K\pi$ • $D \to K3\pi$

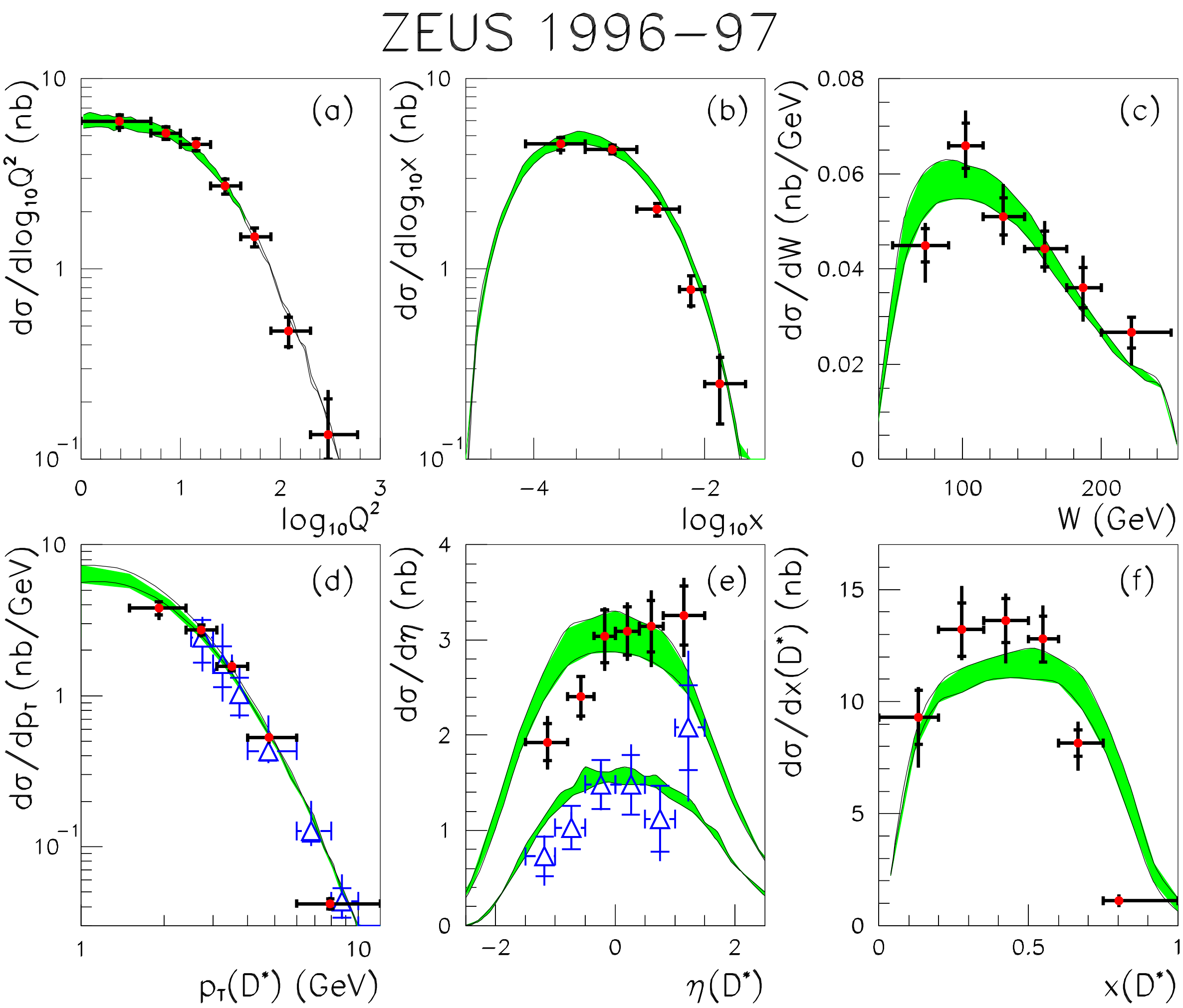

- Calculation based on NLO BGF (HVQDIS, Harris and Smith) for $c\bar{c}$ production

- need fragment. function $c \to D^*$ (0.222, OPAL), branching ratio $D^{*\pm} \to D^0\pi_s^\pm$ (68.3%, PDG)

- important consistency: get the same gluon: global fit to $F_2 \longleftrightarrow$ measured D^* cross sections (these data were not used as input to the NLO DGLAP fit)

Measurement of F_2^c

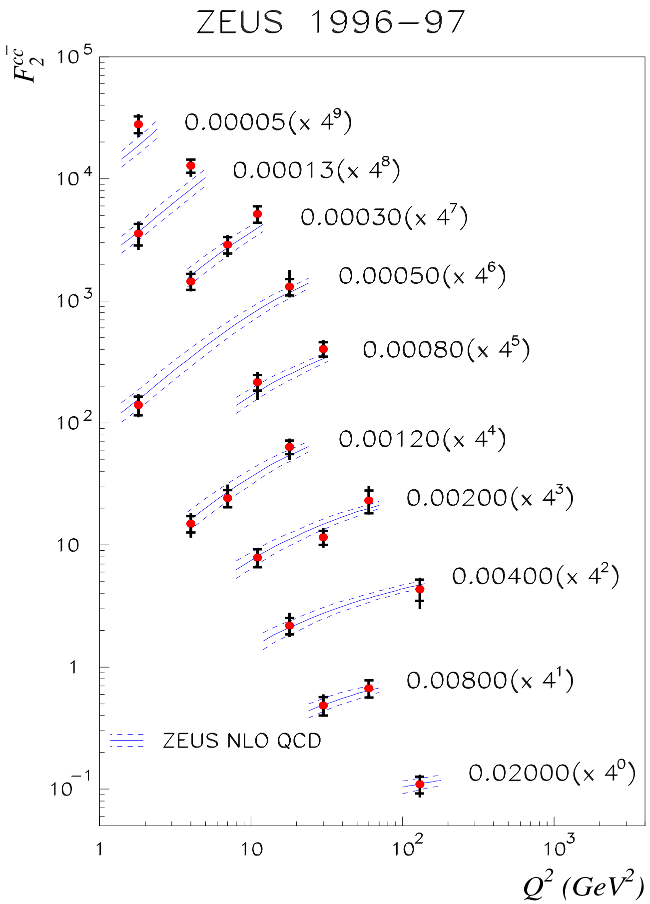

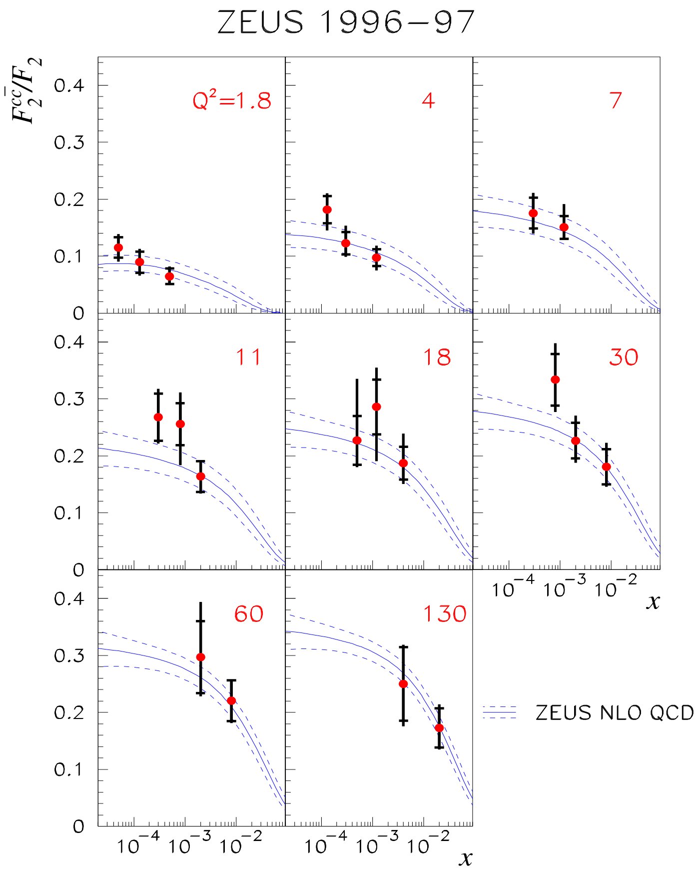

- **Extrapolate to all phase space using NLO to get F_2^c:**
- strong scaling violations ⇒ rising gluon
- the rise of F_2^c is stronger than that of F_2
- the charm content of the proton rises (with Q^2) from ≈ 10% at 1.8 GeV^2 to ≈ 25% at 130 GeV^2

Dijets: gluon distribution

Analysis in the Breit frame; compare to NLO for two renorm. schemes. Mainly BGF process.

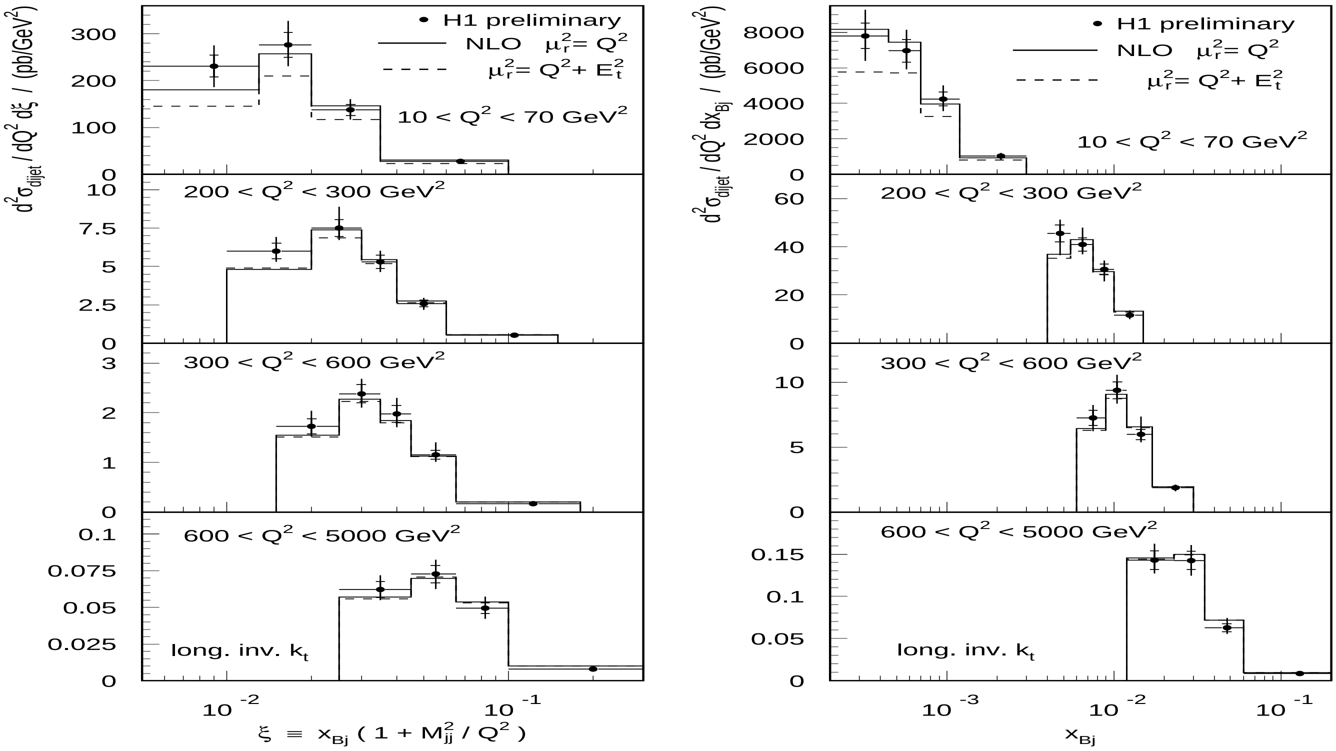

From a NLO QCD fit to the above two cross sections (with quark densities from F_2 data):

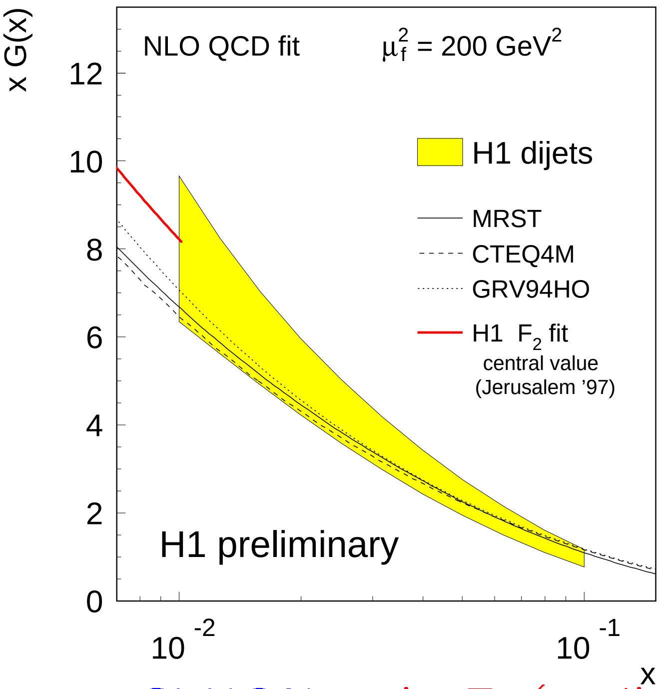

- Get the same GLUON as in F_2 (scaling violations) and F_2^c

Deeply Virtual Compton Scattering

DVCS is the diffractive production of a real photon in DIS. It could provide an indirect measurement of skewed parton distributions. It also allows one to measure the real part of a QCD amplitude.

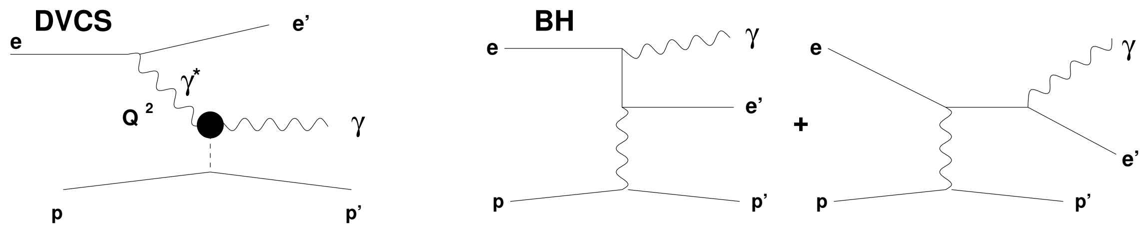

- No final state VM wavefunction to calculate
- BUT Bethe-Heitler (BH) or QED Compton has same final state and so it will interfere with the DVCS amplitude
- DVCS search strategy – look for γ in the 'barrel' region:

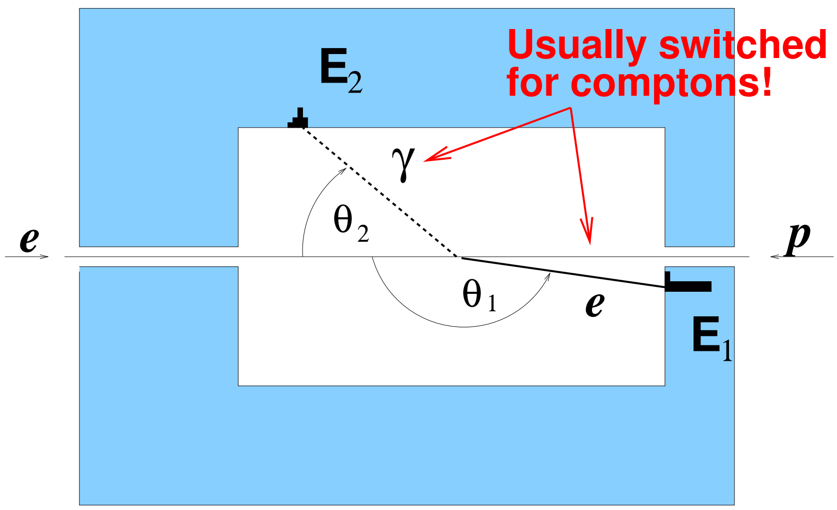

DVCS (2)

Select $Q^2 > 6$ GeV^2 and the energy of the 2nd EM cluster > 2 GeV:

Look at the distributions of the polar angle θ_2 of the 2nd EM cluster:

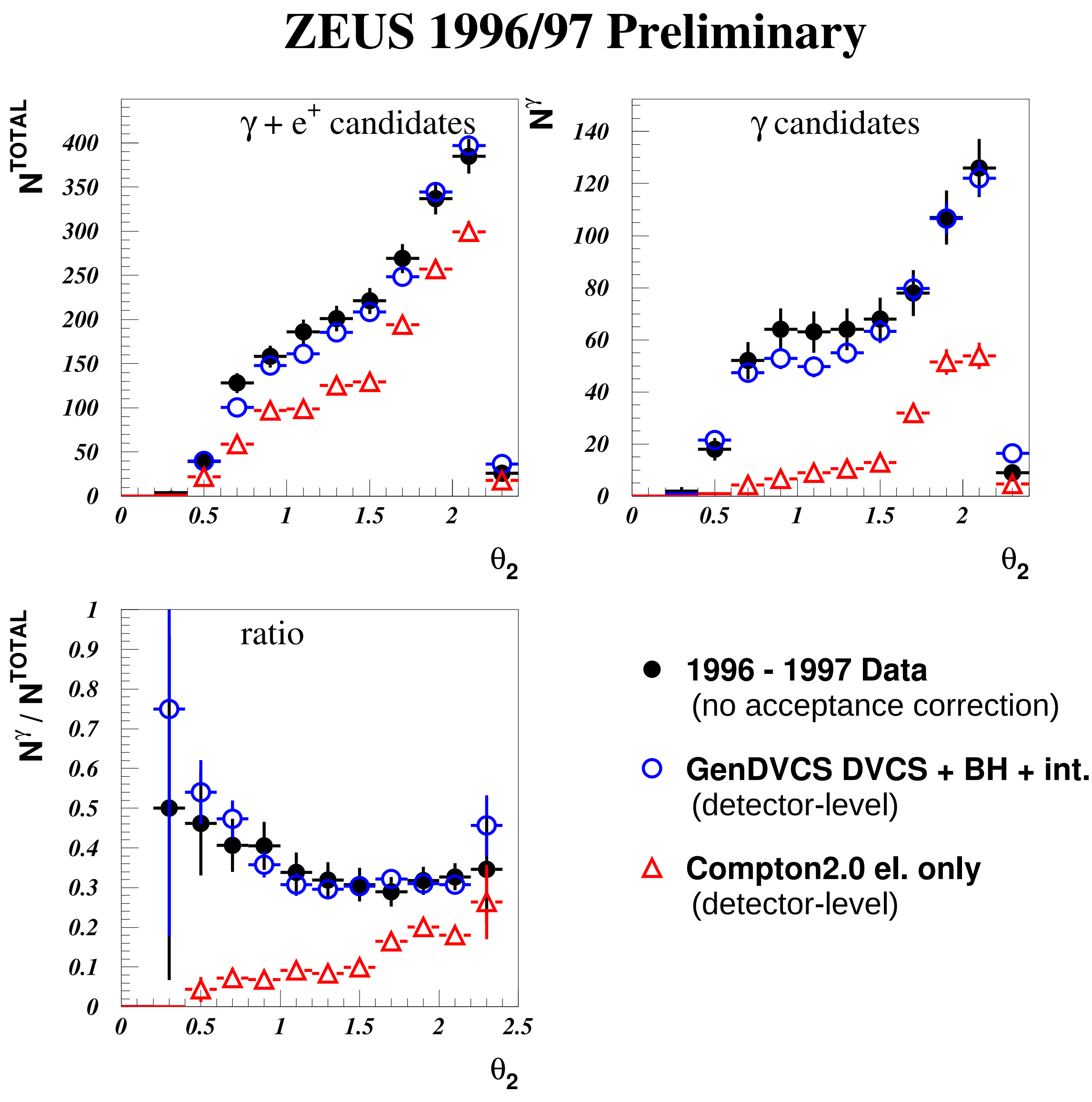

- Distributions are quite different from B-H, hence:
- there appears to be a clear signal for DVCS
- but processes like $ep \to ep\pi^0, ep\pi^0\pi^0$.. could potentially fake this signal ......

DVCS (3)

Study the γ shower shape:

$$Z_{width} = \frac{\Sigma |Z_{cell} - \bar{Z}| \times E_{cell}}{\Sigma E_{cell}}$$

$$f_{MAX} = \frac{Energy\ of\ the\ most\ energetic\ cell\ in\ cluster}{Total\ energy\ in\ the\ cluster}$$

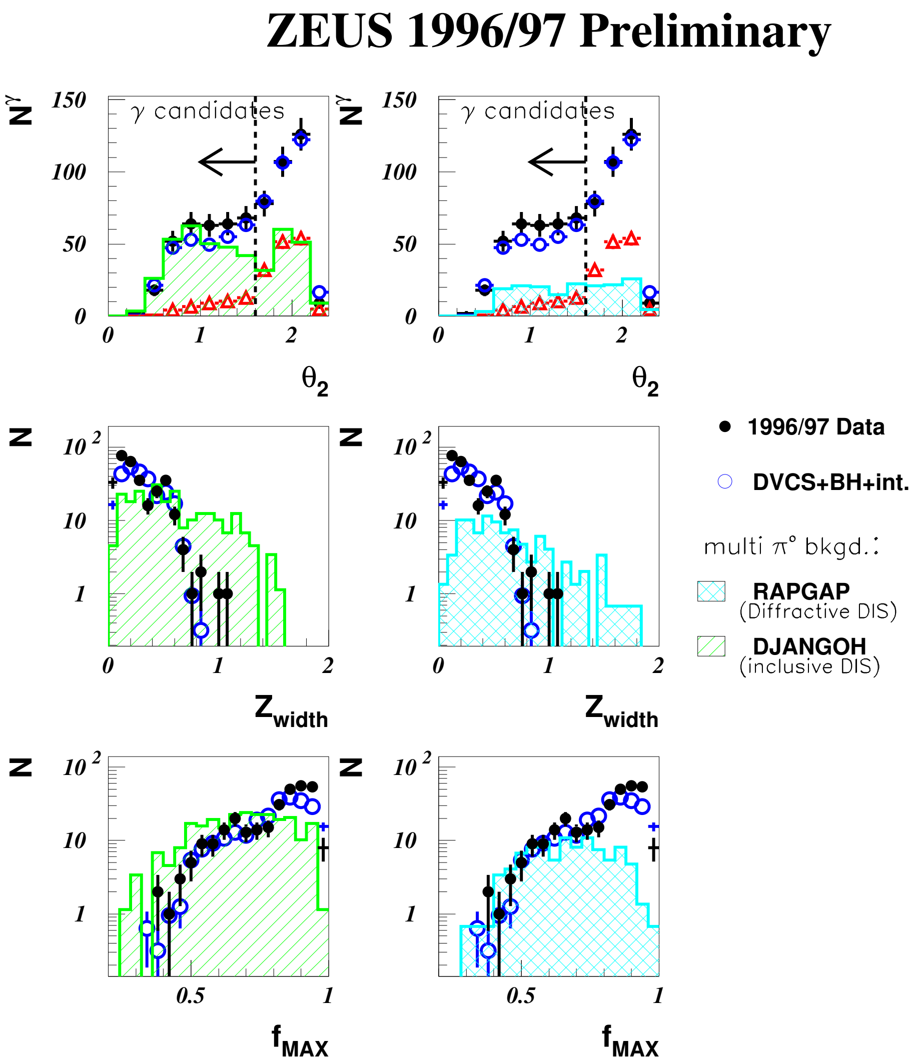

- Conclusion: the π^0/η hypotheses cannot account for the shower shape
- A DVCS-like signal is observed.

Summary

What have we learned from Deep Inelastic Scattering at HERA at medium to high Q^2 ?

- Z^0 ($W^{\pm}$) contributions are observed in NC (CC) reactions in space-like regime.
- Start to distinguish u and d in a single experiment.
- NLO-pQCD fits give a good description of the data. There is no sign of a breakdown of DGLAP even at very low Q^2 ($\sim$ 0.5 GeV^2).
- The pdf's enable us to extrapolate accurately into the high Q^2 regime.
- We get a consistent gluon density from several different processes.

What have we learned from low Q^2 and diffraction:

- We observe a transition from the non-perturbative to the perturbative regime.
- A hard gluon component exists; DGLAP works well here also.
- When a hard scale exists (which can be Q^2, t or M_V^2), $\alpha_{\mathbb{P}}$ increases and flavor independence is approached.

high Q^2 • pQCD $\Longleftrightarrow$ Regge theory • low Q^2

"We need to learn how to make the two live together" (P.V. Landshoff)

Structure functions (1)

Measured quantity in the experiment:

Differential $e^{\pm}p \to e^{\pm}X$ cross section:

$$\boxed{\frac{d^2\sigma(ep \to eX)}{dy\,dQ^2} = \frac{2\pi\alpha^2}{yQ^4}\left(Y_+F_2 - y^2F_L \mp Y_-xF_3\right)(1+\delta_r)}$$

- $Y_{\pm} = 1 \pm (1-y)^2$
- δ_r: radiative corrections

Structure functions of the proton:

- $F_2(x,Q^2) = \sum_q x\,e_q^2\left[q(x,Q^2) + \bar{q}(x,Q^2)\right]$

  $+$ corrections in higher orders QCD

  q, $\bar{q}$: parton density functions

  $$F_2 = F_2^{\mathrm{em}} + \left(\frac{Q^2}{Q^2+M_Z^2}\right)F_2^{\mathrm{int}} + \left(\frac{Q^2}{Q^2+M_Z^2}\right)^2 F_2^{\mathrm{weak}}$$

  "the" structure function of the proton

- $F_L(x,Q^2)$

  at leading order (QPM), $F_L(x,Q^2) = 0$

  calculable from F_2 and gluon density (pQCD)

  small correction, relevant only at high y

  longitudinal structure function

  no direct measurement, but indirect extractions

- $xF_3(x,Q^2)$: negligible for $Q^2 \ll M_Z^2$

  parity violating term

  may be measureable with 1998/99 data

Structure functions (2)

In the following: neglect $xF_3(x, Q^2)$

Reduced cross section:

$$\sigma_r = \frac{d^2\sigma(ep \to eX)}{dy\, dQ^2} \cdot \frac{yQ^4}{2\pi\alpha^2} = F_2 - \frac{y^2}{Y_+} F_L$$

- directly related to measured quantity $\frac{d^2\sigma}{dy\, dQ^2}$

  no uncertainty due to F_L (by construction)

- for $y^2 F_L \ll Y_+ F_2$:

$$\sigma_r \approx F_2$$

- for $y \to 1$:

$$F_L \approx F_2 - \sigma_r$$

Factorization in γ^* flux and $\gamma^* p$ cross section:

$$\boxed{\frac{d^2\sigma(ep \to eX)}{dy\, dQ^2} = \Gamma \cdot \left(\sigma_T^{\gamma^* p} + \epsilon\, \sigma_L^{\gamma^* p}\right) (1 + \delta_r)}$$

- $\Gamma = \alpha Y_+ / 2\pi y Q^2$: virtual photon flux
- $\epsilon = 2(1 - y)/Y_+$: photon polarization
- at low x:

$$\sigma_{\text{tot}}^{\gamma^* p} = \sigma_T^{\gamma^* p} + \sigma_L^{\gamma^* p} \approx \frac{4\pi^2 \alpha}{Q^2} F_2$$

Q^2-evolution of F_2

DGLAP equations (NLO-pQCD):

- predict evolution of parton densities with Q^2
- no prediction of x dependence

$$\boxed{\begin{aligned} \frac{dg}{d\ln Q^2} &= \frac{\alpha_s(Q^2)}{2\pi}(P_{gg}\otimes g + P_{gq}\otimes q) \\ \frac{dq}{d\ln Q^2} &= \frac{\alpha_s(Q^2)}{2\pi}(P_{qg}\otimes g + P_{qq}\otimes q) \end{aligned}}$$

- q_i: quark densities $q = \sum_i q_i$
- g: gluon density
- convolution $P_{ij}\otimes f = \int_x^1 \frac{dx'}{x'} f(x',Q^2) P_{ij}\left(\frac{x}{x'}\right)$

Splitting functions P_{ij}:

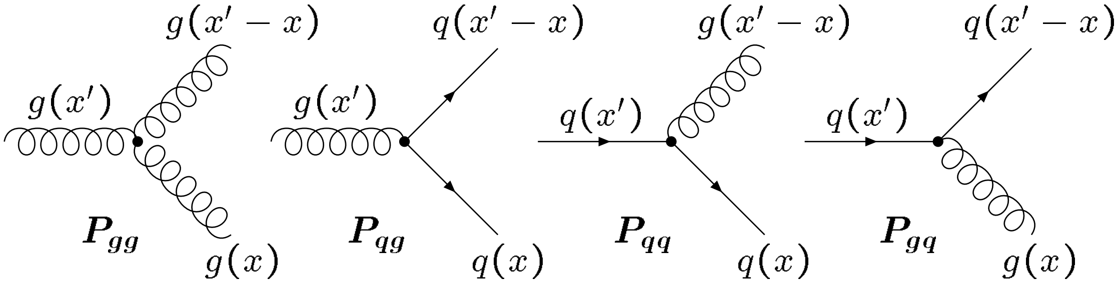

- valence quarks at high x radiate gluons
- gluons split $\rightarrow$ more gluons at low x
  $\rightarrow$ sea quark-antiquark pair at low x
- higher Q^2 = higher resolving power:
  photon starts to "see" radiation and splitting
  increase of F_2 at low $x \Longleftrightarrow$ decrease at high x

DGLAP fits

DGLAP fits (NLO-pQCD):

- parameterize quark and gluon densities at Q_0^2: (e.g. MRST, similar for ZEUS and H1)
  - gluon: xg
    $xg(x, Q_0^2) = A_g x^{\delta_g}(1-x)^{\eta_g}(1+\epsilon_g\sqrt{x}\gamma_g x)$
  - sea quarks: $2x(\bar{u}+\bar{d}+\bar{s})$
    $xS(x, Q_0^2) = A_s x^{\delta_s}(1-x)^{\eta_s}(1+\epsilon_s\sqrt{x}+\gamma_s x)$
  - difference Up – Down: $x(u+\bar{u}-d-\bar{d})$
    $x\Delta(x, Q_0^2) = A_\Delta x^{\eta_\Delta}(1-x)^{\eta_\Delta+2}(1+\gamma_\Delta x+\delta_\Delta x^2)$
  - valence quarks: $x(u-\bar{u})$ and $x(d-\bar{d})$
    $xu_v(x, Q_0^2) = A_u x^{\delta_u}(1-x)^{\eta_u}(1+\epsilon_u\sqrt{x}+\gamma_u x)$
    $xd_v(x, Q_0^2) = A_d x^{\delta_d}(1-x)^{\eta_d}(1+\epsilon_d\sqrt{x}+\gamma_d x)$
- impose momentum sum rule $\rightarrow$ fix one parameter
- use DGLAP equations to evolve to all Q^2, calculate F_2
- adjust free parameters to fit data for $Q^2 > Q^2_{\mathrm{min}}$

Choice of scales:

- Q_0^2: in principle arbitrary, usually $\approx 1-10\,\mathrm{GeV}^2$
  (analytic parameterization should fit F_2 at Q_0^2)
- Q^2_{min}: cut-off above which pQCD is applicable

$\rightarrow$ can DGLAP fit describe the data for all Q^2 ?

ZEUS detector

Structure function measurement: inclusive cross section measurement with tagged scattered e'

ideal situation: require a track, measure energy in calorimeter ($\rightarrow$ good positron identification & detection)

$e \longrightarrow$
27.5
GeV

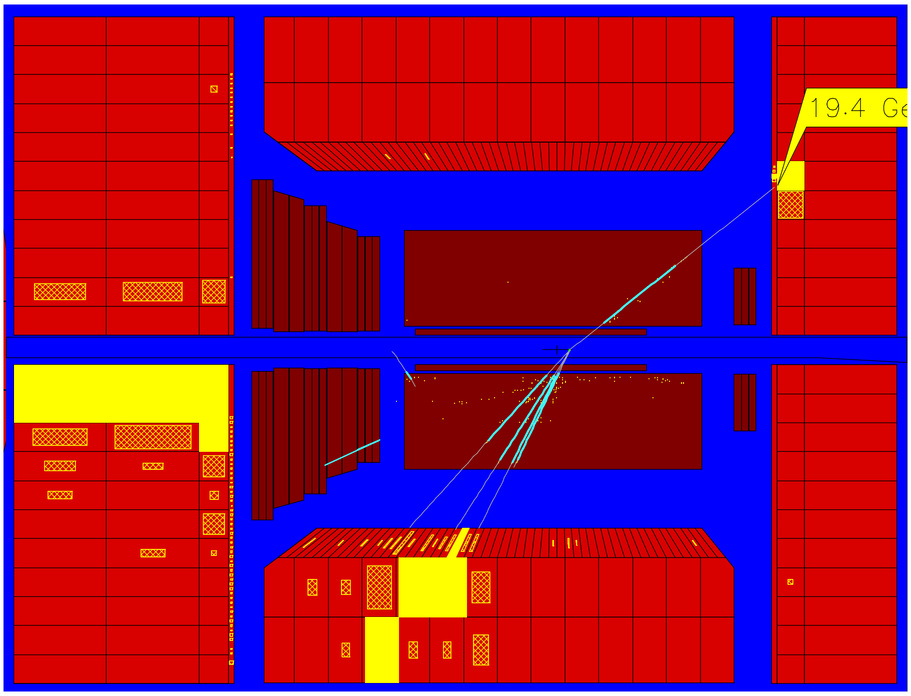

$\longleftarrow p$
820
GeV

CAL **Uranium Calorimeter**

- uranium-scintillator sandwich calorimeter
- acceptance: $5^o < \theta < 174^o$

CTD **Central Tracking Detector**

- cylindrical drift chamber
- acceptance: $16^o < \theta < 165^o$

$\rightarrow$ no tracking at low scattering angles

H1 detector

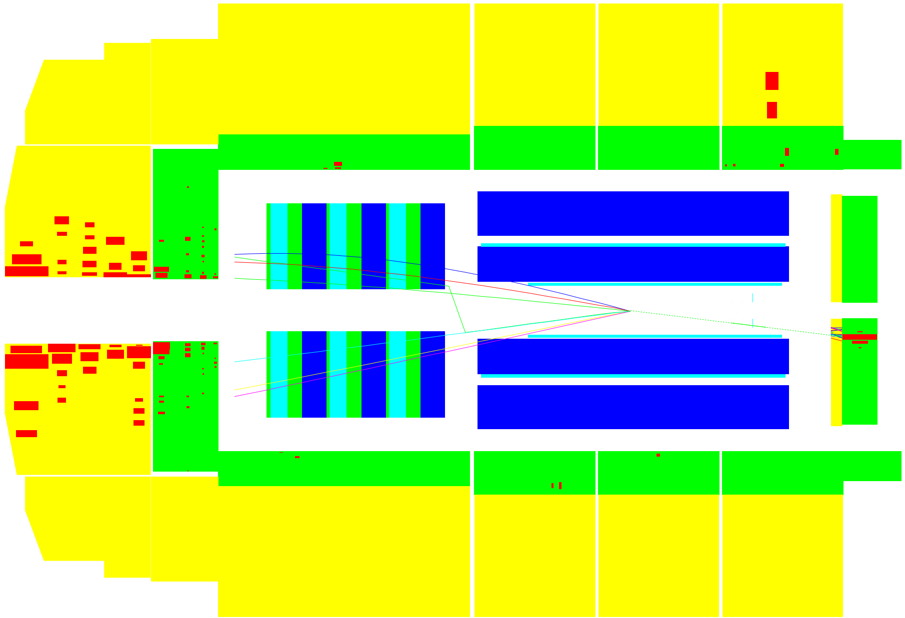

SPACAL **Spaghetti Calorimeter**

- lead-scintillating fiber calorimeter

BDC **Backward Drift Chamber**

- 8 layer drift chamber

BST **Backward Silicon Tracker, new in 1997**

- 4 rear discs (part of silicon microvertex detector)
- acceptance: $3^{\circ} < \theta < 8^{\circ}$

$\rightarrow$ Special tracking detectors for low angles

ZEUS detector

Access to low Q^2 ($< 1\,\mathrm{GeV}^2$): special detectors as close as possible to the beam line

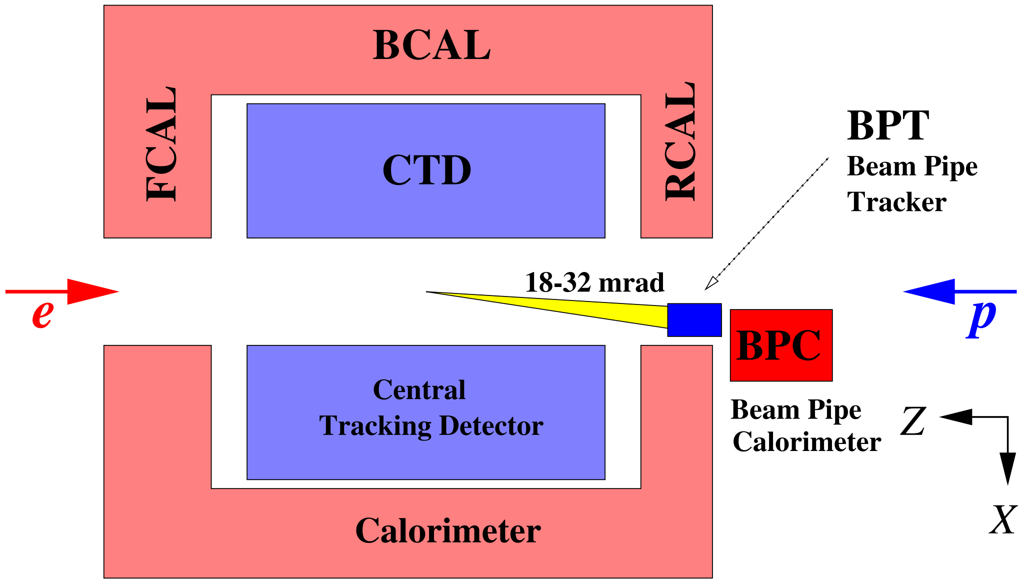

BPC **Beam Pipe Calorimeter**

- tungsten-scintillator sampling calorimeter

BPT **Beam Pipe Tracker, new in 1997**

- 2 silicon microstrip detectors
- acceptance: $1.1° < \theta < 1.9°$

for $Q^2 \approx 0$: taggers along beam line (H1+ZEUS)